Review of "Investigation of CATS aerosol products and application toward global diurnal variation of aerosols" by Logan Lee, Jianglong Zhang, Jeffrey S. Reid, and John E. Yorks

reviewed by Mark Vaughan

This paper compares the spatial and temporal distributions of the aerosol optical depths retrieved at 1064 nm by the CATS lidar aboard the International Space Station to the optical depths measured by AERONET (at 1020 nm) and the optical depths retrieved by MODIS and CALIOP (at 1064 nm).

This is the second version of this manuscript that I have read, but the first for which I've been asked to provide an invited (as opposed to contributed) review.

My primary comment about this second version is that the authors' do not provide enough information for readers to confidently assess the quality of the CATS AOD estimates relative to those provided by the other sensors. In particular, relying on correlation coefficients alone to characterize the comparisons is insufficient. Consider the two series defined by $y_2 = 2x$ and $y_4 = 4x$. While y_2 and y_4 are perfectly correlated – i.e., they have a correlation coefficient of 1 – in the mean, y_4 is twice as large as y_2. So in addition to the correlation coefficients they already provide, the authors should also provide means and standard deviations for each of the datasets being compared. While Table 2 is a fine start, more is needed.

In a similar vein, regarding figures 1 through 3, black-on-black overplotting of data points in high data density regions reduces the information content of the figures. So, in addition to the figures, the authors should also cite the descriptive statistics (e.g., min, max, median, mean, and standard deviation) for all datasets being compared. Furthermore, optical depths should be given (either in the text or, preferably, in the figure captions or legends) for all profiles plotted in figure 5 and figures 10–13.

It is also my view that the authors have not responded sufficiently to several of the comments made by the original referees. Below I have listed the original referee comments together with the authors' responses and my criticisms of those responses. I hope the authors will revisit their original responses, and consider adding the additional requested by all referees.

In addition to this review, I have attached an annotated version of the manuscript that contains a number of questions and suggestions. I hope to see responses to these issues reflected in the published version of this paper.

Referee 1:

Comments: Specific comments: Section 2, can you briefly describe the AOD measurement uncertainty of these instrument?

Response: This is a great question. Most validation and uncertainties analysis efforts of satellite AOD retrievals are focus on visible channels. To our knowledge, uncertainties in AOD retrieval at 1064 nm, both from passive and active sensors, are less studied. Just as suggested from the comments from Mark Vaughan and Stuart Young (Short comment for this paper), this paper might be among the first to go deep into AOD retrievals at 1064 nm channel. We were not able to find *papers to address uncertainties in AOD retrievals at 1064 nm, although there are papers that do show comparisons between CALIOP and AERONET AOD at 1064 nm (Omar et al., 2013).*

Omar, A. H., D. M. Winker, J. L. Tackett, D. M. Giles, J. Kar, Z. Liu, M. A. Vaughan, K. A. Powell, and C. R. Trepte (2013), CALIOP and AERONET aerosol optical depth comparisons: One size fits none, J. Geophys. Res.Atmos.,118, 4748–4766, doi:10.1002/jgrd.50330.

We have added the following discussion in the text: "Note that most evaluation efforts for passive- and active-based AOD retrievals are focused on the visible spectrum and the performance of AOD retrievals at the 1064 nm channel is less explored. "

I don't think this response adequately addresses reviewer's request. Estimating measurement uncertainties in not synonymous with validation; ideally, the former would always precede the latter. MODIS AOD uncertainties are explored in numerous papers (e.g., Tanré et al., 1997; Levy et al., 2003; Remer et al., 2005; and many others), and the same is true for AERONET aerosol retrievals (e.g., Holben et al., 1998; Dubovik et al., 2000; Sinyuk et al., 2012; and many others). Uncertainties in extinction and optical depth estimates retrieved using elastic backscatter lidars have a long history in the literature (e.g., Russell et al., 1997; Bissonnette, 1986; Jinhuan, 1988; Young, 1995; Del Guasta, 1998). In particular, the retrieval uncertainties for CALIOP are given in excruciating detail in Young et al., 2013. I'm not aware of any publication that specifically examines CATS extinction uncertainties. However, since CALIOP and CATS are both elastic backscatter lidars that use similar retrieval algorithms, I suspect that the material in Young et al., 2013 could easily be adapted to provide first-order estimates for the CATS uncertainties.

I suspect the authors could make a useful response to this referee's request in just 3 or 4 summary sentences.

<u>References</u>

Bissonnette, L. R., 1986: Sensitivity analysis of lidar inversion algorithms, Appl. Opt., 25, 2122–2125, doi:10.1364/AO.25.002122.

Del Guasta, M., 1998: Errors in the retrieval of thin-cloud optical parameters obtained with a two-boundary algorithm, Appl. Opt., 37, 5522–5540, doi:10.1364/AO.37.005522.

Dubovik, O., A. Smirnov, B. N. Holben, M. D. King, Y. J. Kaufman, T. F. Eck, and I. Slutsker, 2000: Accuracy assessments of aerosol optical properties retrieved from Aerosol Robotic Network (AERONET) Sun and sky radiance measurements, J. Geophys. Res., 105, 9791– 9806, doi:10.1029/2000JD900040.

Holben, B. N., T. F. Eck, I. Slutsker, D. Tanre, J.P. Buis, A. Setzer, E. Vermote, J. A. Reagan, Y. J. Kaufman, T. Nakajima, F. Lavenu, I. Jankowiak and A. Smirnov, 1998: AERONET — A federated instrument network and data archive for aerosol characterization, Rem. Sens. Env., 66, 1-16, doi:10.1016/S0034-4257(98)00031-5.

Jinhuan, Q., 1988: Sensitivity of lidar equation solution to boundary values and determination of the values, Adv. Atmos. Sci., 5, 229–241, doi:10.1007/BF02656784.

Levy, R. C., L. A. Remer, D. Tanré, Y. J. Kaufman, C. Ichoku, B. N. Holben, J. M. Livingston, P. B. Russell and H. Maring, 2003: Evaluation of the Moderate-Resolution Imaging Spectroradiometer (MODIS) retrievals of dust aerosol over the ocean during PRIDE, J. Geophys. Res., 108, 8594, doi:10.1029/2002JD002460.

Remer, L. A., Y. J. Kaufman, D. Tanre, S. Mattoo, D. A. Chu, Martins, J. V., Li, R. R., Ichoku, C., Levy, R. C., R. G. Kleidman, T. F. Eck, E. Vermote, and B. N. Holben , 2005: The MODIS aerosol algorithm, products, and validation, J. Atmos. Sci., 62, 947–973, doi:10.1175/JAS3385.1.

Russell, P. B., T. J. Swissler, and M. P. McCormick, 1979: Methodology for error analysis and simulation of lidar aerosol measurements, Appl. Opt., 22, 3783–3797, doi:10.1364/AO.18.003783.

Sinyuk, A., B. N. Holben, A. Smirnov, T. F. Eck, I. Slutsker, J. S. Schafer, D. M. Giles and M. Sorokin, 2012: Assessment of error in aerosol optical depth measured by AERONET due to aerosol forward scattering, Geophys. Res. Lett., 39, L23806, doi:10.1029/2012GL053894.

Tanré, D., Y. J. Kaufman, M. Herman and S. Mattoo, 1997: Remote sensing of aerosol properties over oceans using the MODIS/EOS spectral radiances, J. Geophys. Res., 102 (D14), 16971–16988, doi:10.1029/96JD03437.

Young, S. A., 1995: Analysis of lidar backscatter profiles in optically thin clouds, Appl. Opt., 34, 7019-7031, doi:10.1364/AO.34.007019.

Young, S. A., M. A. Vaughan, R. E. Kuehn, and D. M. Winker, 2013: The Retrieval of Profiles of Particulate Extinction from Cloud-Aerosol Lidar Infrared Pathfinder Satellite Observations (CALIPSO) Data: Uncertainty and Error Sensitivity Analyses, J. Atmos. Oceanic Technol., 30, 395-428, doi:10.1175/JTECH-D-12-00046.1.

Comments: P8, L163, can you describe what constant value of that Angstrom exponent is used here without letting readers to look for that in Shi et al. paper?

Response: We apologize for the confusion. The Angstrom exponent values are computed using instantaneous retrievals. We have revised the text to avoid confusion.

"Here we assume the angstrom exponent value, computed using instantaneous AOD retrievals at the 860 and 1240 nm, remains the same for the 860 to 1064 nm wavelength range, similar to what has been suggested by Shi et al., (2011; 2013)."

Please provide a representative range (e.g., mean and standard deviation or some other common statistical description) of the Ångström exponents actually used.

Comments: Can you provide an explanation on why the AOD measured by CATS less than all other instruments suggested by Figure 1, 2, and 3?

Response: We assume that the reviewer is referring to the slope of the regressions in Figures 1-3. Slopes in linear regressions can often be biased by outliers. In Figure 6, which are spatial plots of AODs from CALIOP and CATS, differences are less noticeable for the DJFMAM season.

For the JJASON season, CATS AODs are lower at certain regions (Middle East, India, and North Africa) and higher over other regions (South Africa). The cause of those discrepancies, however, is unclear to us. To really explore the issue, it deserves a paper of its own. Thus, we leave this topic to a future paper

I'm quite perplexed by this response. First, if the slopes are not trustworthy indicators of the correlation between the two data sets, why report them at all? Or, if the authors are concerned that "slopes in linear regressions can often be biased by outliers", why didn't they remove any obvious outliers before plotting their data and computing and reporting the values of the slopes?

Second, and perhaps more important, there's at least one plausible and obvious answer to the reviewer's question. According to Rebecca Pauly's CATS calibration paper, the CATS attenuated backscatter coefficients are biased low by ~19% relative both to ground-based Polly^{XT} measurements and to CALIOP measurements. This low bias in the attenuated backscatter coefficients will invariably lead to low biases in the retrieved optical depths (see the section on calibration and renormalization errors in Young et al., 2013).

(Full disclosure: I am a back-of-the-pack coauthor on Rebecca Pauly's CATS calibration paper.)

In my opinion, this comment should be fully addressed in this paper, and not postponed to some future paper. There are several reasons why "the AOD measured by CATS [might be] less than all other instruments", and the authors should make a good faith attempt to enumerate and discuss at least the most obvious of those reasons.

Referee 2:

Comments: (5) The aerosol extinction at 1064 nm may not be as sensitive to the fine mode aerosols (such as smoke and urban pollutant aerosols) compared to the coarse mode aerosols (such as dust). The authors probably should add a few sentences to address this

*Response: Great point. We have added the following discussions to address this issue. "Still, readers ~~shall~~ **should** be aware that AOD retrievals at the 1064 nm are less sensitive to fine mode aerosols such as smoke and pollutant aerosols, compared to coarse mode aerosols such as dust aerosols. Thus, an investigation of diurnal variations of aerosol properties at the visible channel may be also needed for a future study."*

A reference for the first statement would make a very nice addition to the paper.

Short Comments by Mark Vaughan and Stuart Young

Comment: While the main body of the text emphasizes the correlations between the CATS retrievals and the other data sets (e.g., lines 186–208), the authors do not provide any quantitative statements about the magnitudes of the CATS AODs or the differences between the different AOD estimates. Given that this paper is (to our knowledge) the first ever in-depth look at 1064 nm AOD, tables showing global and regional mean values and quantifying the CATS AOD estimates relative to the other sensors would add significantly to the value delivered by this paper. Profiles of the relative CATS-CALIOP extinction coefficient differences (i.e., (CATS(z) - CALIOP(z)) / CALIOP(z)) would be especially interesting.

Response: We have added a table to include regional and global means. Still, we documented that the differences may also be introduced by sampling differences of the sensors.

"Table 2. CALIOP and CATS mean aerosol optical depth for regions as highlighted in Figure 6 and globally between +/- 52° latitude."

Region	*Latitude*	*Longitude*	*Mean CATS AOD (DJFMAM/JJASON)*	*Mean CALIOP AOD (DJFMAM/JJASON)*
Global	*52°S-52°N*	*180°W-180°E*	*0.09/0.10*	*0.09/0.09*
India	*7.5°N - 32.5°N*	*65°E - 85°E*	*0.22/0.26*	*0.22 /0.28*
Africa - North	*2.5°N - 22.5°N*	*35°W - 20°E*	*0.26/0.23*	*0.30 /0.25*
Africa - South	*17.5°S - 2.5°N*	*0° - 30°E*	*0.14/0.22*	*0.15 /0.13*
Middle East	*12.5°N - 27.5°N*	*35°E - 50°E*	*0.22/0.33*	*0. 26/0.35*
China	*27.5°N - 37.5°N*	*110°E - 120°E*	*0.19/0.18*	*0.21 /0.16*

I strongly suggest adding standard deviations to this table; the observed variability of the AODs provides a critically important point of comparison between the two sets of retrievals. I also suggest adding a table comparing CATS means and standard deviations to the AERONET and MODIS means and standard deviations.

Comment: In section 3.1.1., CATS observations are compared with other observations made within ±30 mins and ±0.4 degrees. For aerosols, this is probably not too much of a problem a lot of the time, but we have seen numerous cases where there can be large differences in the scenes being observed (e.g., see Omar et al., 2013: "In 45% of the coincident instances CALIOP and AERONET do not agree on the cloudiness of the scenes."). For AERONET, the comparisons may be improved by imposing another criterion, i.e., that the AERONET AODs made at the closest times preceding and following the CATS observations not vary by more than x%. A similar filter for potential spatial differences could include wind speed and direction (e.g., Lopes et al., 2013) and the spatial separations of the AERONET sites and the CATS observations. (This is likely to be quite a bit messier.)

Response: We have included the references as suggested and reminded readers that the collocation criteria may have impacts to the results due to the spatial and temporal sampling methods chosen.

"Note that as suggested by Omar et al., 2013, the choices of spatial and temporal collocation windows have an effect on collocation results. ***However, we consider this as a topic beyond the scope of this study***"

While I did not expect the authors to do a complete reanalysis of their data, I had hoped to see a bit more in-depth discussion of the uncertainties inherent in this kind of simple temporal and spatial matching technique and some discussion, perhaps, on how these might be mitigated. For example, the authors use version 3 level 2 AERONET data in their study, whereas the Omar et al., 2013 analysis used version 2 level 2 AERONET data. Are there improvements between versions 2 and 3 that might reduce the differences in the cloudiness inferred by AERONET versus the cloudiness observed by coincident space-based lidar measurements?

Comment: Furthermore, given the lower CATS AODs shown in Figure 2, it's surprising to see that the CATS extinctions coefficients shown in Figure 5 are typically larger than CALIOP at all altitudes, and that the closest agreement is over land (where CATS slightly underestimates

CALIOP at lower altitudes). Again, some discussion of the possible causes of this paradox would be welcome.

Response: First, there is a call from the community to avoid using slopes from the regression analysis as they are prone to noisy data, and we are kind of agree with them. Statistically, we expect a high percentage of small AODs versus large AODs. Still, slopes are dominated by high AOD cases, while the averaged profiles may be more dominated by low AOD cases. This could explain the difference.

This response helped motivate my "primary comment" in the opening paragraphs of this review. Given that slopes (and correlation coefficients) are imperfect metrics, additional statistical parameters should be given to more fully characterize the comparisons between the different datasets.

Comment: The CATS extinction profiles shown in Figures 5 and 10 peak at altitudes some hundreds of meters higher than do CALIOP's, except over land. While CALIOP's profiles show almost no roll off until about the last range bin above the surface, the CATS profiles start dropping off below about 500 m, or at approximately 8 to 9 range bins above the surface. What is happening here? Is CATS altitude registration and/or surface detection the culprit? Or is the cloud filter too aggressive in the boundary layer (i.e., are strongly scattering aerosols being misclassified as clouds)? Irrespective of the underlying cause(s), is this behavior a major source of AOD differences between CATS and CALIOP?

Response: The 2 biggest issues in the CATS V2-01 data were the daytime calibration and the daytime cloud-aerosol discrimination. A CATS paper in preparation (Yorks et al., 2019) has included details about the cloud-aerosol discrimination issues, while Rebecca Pauly's 1064 nm calibration paper has a lot of details about the new daytime calibration. We have checked this issue by reprocessing the analysis using 3 months of V3 data and we found an improvement in agreement for AOD, but with some differences still evident in the vertical profiles.

While this is a helpful explanation, I do not see where it appears in the revised paper. Given that the CATS V3 data is now publicly available, I think it's essential to include some information that relates these findings to the currently available CATS data.

Comment: The seasonal maps (Figure 6) show that the CALIOP AODs exceed those of CATS over the Arabian Peninsula, and to a smaller degree over the African region bordering the Gulf of Guinea. Can this also be explained by differences in lidar ratio selection, or are there other factors at work?

Response: We suspect the difference in retrieval method as mentioned above may contribute. Also, CALIOP provides early morning and afternoon overpasses while CATS can observe at near all solar hours, the differences may also be associated with these sampling differences.

Again, I do not see where this helpful explanation appears in the revised manuscript.

Specific Comments

Comment: page 8, line 163: logarithmic interpolation, correct? Also, please state the actual value of the Ångström exponent given by Shi et al.

Response: Yes. The Angstrom exponent value is computed for each AOD retrieval. We have revised the discussion to avoid confusion. "Here we assume the angstrom exponent value, computed using *instantaneous AOD retrievals at the 860 and 1240 nm, remains the same for the 860 to 1064 nm wavelength range, similar to what has been suggested by Shi et al., (2011; 2013)."*

To repeat an earlier comment, please provide a representative range (e.g., mean and standard deviation or some other common statistical description) of the Ångström exponents actually used. Don't leave your readers guessing and/or wondering about what values you used in deriving your 1064 nm AOD estimates.

Comment: page 8, line 170: while "AERONET data are considered as the ground truth for evaluating CATS retrievals", it should be noted that there are very few AERONET sites in remote oceans. Do MODIS retrievals substitute as the gold standard in these places?

Response: Even though a better performance can be expected from MODIS aerosol retrievals over ocean versus over land, we still think that only AERONET data should be used for ground truth, as instantaneous retrievals from passive sensors suffer from various issues such as cloud contamination.

This is not a very useful response, mostly because AERONET, like MODIS, is a passive sensor and thus also suffers from "various issues such as cloud contamination" (e.g., Chew et al., 2011 and Huang et al., 2011).

Taking the authors' response at face value, the number of opportunities for ground truth over ocean must be vanishingly small relative to the number of over-ocean measurements being evaluated.

References

Chew et al., 2011: Tropical cirrus cloud contamination in sun photometer data, Atmos. Environ., 45, 6724-6731, https://doi.org/10.1016/j.atmosenv.2011.08.017

Huang et al., 2011: Susceptibility of aerosol optical thickness retrievals to thin cirrus contamination during the BASE-ASIA campaign J. Geophys. Res., 116, D08214, doi:10.1029/2010JD014910.

Comment: page 9, line 186-187: some discussion on the rationale for the choices of ±0.4° and ±30 minutes would be helpful in evaluating the strength of the comparisons.

Reponses: We picked this threshold following a few previous papers (e.g. Toth et al., 2018). We have added discussions in the text to further clear this issue:

"Note that as suggested by Omar et al., 2013, the choices of spatial and temporal collocation windows have an effect on collocation results. However, we consider this as a topic beyond the scope of this study"

See my previous remarks on this response.

Investigation of CATS aerosol products and application toward global diurnal variation of aerosols

Logan Lee[1], Jianglong Zhang[1], Jeffrey S. Reid[2], and John E. Yorks[3]

[1]Department of Atmospheric Sciences, University of North Dakota, Grand Forks, ND

[2]Marine Meteorology Division, Naval Research Laboratory, Monterey, CA

[3]NASA Goddard Space Flight Center, Greenbelt, MD

Submitted to

ACP

Dec. 2018

Corresponding Author: jzhang@atmos.und.edu; logan.p.lee@und.edu

Abstract

We present a comparison of 1064 nm aerosol optical depth (AOD) and aerosol extinction profiles from the Cloud-Aerosol Transport System (CATS) Level 2 aerosol product with collocated Aerosol Robotic Network (AERONET) AOD, Aqua and Terra Moderate Imaging Spectroradiometer (MODIS) Dark Target (AOD) and Cloud-Aerosol Lidar with Orthogonal Polarization (CALIOP) AOD and extinction data for the period of Feb. 2015-Oct. 2017. Upon quality assurance checks of CATS data, reasonable agreements are found between aerosol data from CATS and other sensors. Using quality assured CATS aerosol data, for the first time, variations in AODs and aerosol extinction profiles are evaluated at 00, 06, 12, and 18 UTC (and/or 0:00 am, 6:00 am, 12:00 pm and 6:00 pm local solar times) on both regional and global scales. This study suggests that marginal variations are found in AOD from a global mean perspective, with the maximum and minimum aerosol vertical profiles found at local noon and 6:00 pm local time respectively, for both the June-November and December-May seasons. Strong diurnal variations are found over North Africa and India for the December-May season, and over North Africa, Middle East, and India for the June-November season. In particular, over North Africa, during the June-November season, a diurnal peak in aerosol extinction profile of 20% larger than daily mean is found at 6:00 am (early morning local time), which may possibly be associated with dust generation through the breaking down of low level jet during morning hours.

1.0 Introduction

Aerosol measurement through the sun-synchronous orbits of Terra and Aqua by nature encourages a larger scale, daily average point of view. Yet, we know that pollution (e.g., Zhao et al., 2009; Tiwarl et al., 2013; Kaku et al., 2018), fires and smoke properties (e.g., Reid et al., 1999; Giglio et al., 2003; Hyer et al., 2013), and dust (e.g., Mbourou, et al., 1997; Fielder et al., 2013; Heinold et al., 2013) can exhibit strong diurnal behavior. Sun-synchronous passive satellite aerosol observations from the solar spectrum only provide a small sampling of the full diurnal cycle and geostationary sensors such as the Advanced Himawari Imager (AHI) on Himawari 8 (Yoshida et al., 2018) and Advanced baseline Imager on GOES-16/17 (Aerosol Product Application Team of the AWG Aerosols/Air Quality/Atmospheric Chemistry Team, 2012) satellites, while an improvement over their predecessors, must overcome the broader range of scattering and zenith angles (Wang et al., 2003; Christopher and Zhang, 2002) with no nighttime retrievals. AErosol RObotic NETwork (AERONET; Holben et al., 1998) based sun photometer studies improve sampling, but until very recently with the development of a prototype lunar photometry mode, are also limited to daylight hours. The critical early morning and evening are largely missed in solar observation based approaches.

Observation-based diurnal variations of aerosol properties are needed for improving chemical transport modeling, geochemical cycles and ultimately climate. The measurement of diurnal variations of aerosol properties resolved in the vertical is especially crucial of aerosol phenomena for visibility and particulate matter forecasts. Indeed, the periods around sunrise and sunset show significant near surface variability that is difficult to detect with passive sensors. While lidar data from Cloud-Aerosol Lidar with Orthogonal Polarization (CALIOP) provide early afternoon and morning observations, two temporal points and a 16 day repeat cycle are insufficient to evaluate the morning and evening hours.

Some of the limiting factors in previous studies can be addressed by the Cloud-Aerosol Transport System (CATS) lidar flying aboard the International Space Station (ISS) since 2015 (McGill et al. 2015). The ISS's precessing orbit with a 51.6° inclination allows for 24 hour sampling of the tropics to mid-latitudes, with the ability to observe aerosol and cloud vertical distributions at both day and night time with high temporal resolution. For a given location within ±51.6° (Latitude), after aggregating roughly 60 days of data, near full diurnal cycle of aerosol and cloud properties can be obtained from CATS observations (Yorks et al. 2016). This provides a new opportunity for studying diurnal variations (day and night) in aerosol vertical distributions from space observations.

Use of CATS has its own challenges. Most importantly, CATS retrievals must cope with variable solar noise around the terminator where we expect the strongest diurnal variability to exist. Further, CATS lost its 532 nm channel early in its deployment, leaving only a 1064 nm channel functioning. The availability of only one wavelength limited the CATS cloud-aerosol discrimination algorithm, which can cause a loss of accuracy compared to CALIPSO which has 2 wavelengths. This deficiency is in part overcome by using the Feature Type Score (CATS Algorithm Theoretical Basis Document). Using two years of observations from CATS, in this paper, we focus on understanding of the following questions: How well do CATS derived aerosol optical depth (AOD) and aerosol vertical distributions compare with aerosol properties derived from other ground-based and satellite observations such as AERONET, MODIS and CALIOP? Do differences exhibit a diurnal cycle? What are the diurnal variations of aerosol optical depth on a global domain? What are the diurnal variations of aerosol vertical distribution on both regional and global scales?

2.0 Datasets

Four datasets, including ground-based AERONET data, as well as satellite retrieved aerosol properties from MODIS and CALIOP, are used for inter-comparing with AOD and aerosol vertical distributions from CATS. Upon thorough evaluation and quality assurance procedures, CATS data are further used for studying diurnal variations of AOD and aerosol vertical distributions for the period of Feb. 2015 – Oct. 2017.

2.1 CATS

CATS Level 2 (L2) Version 2-01 5 km Aerosol Profile products (L20_D-M7.2-V2-01_5kmPro, L20_N-M7.2-V2-01_5kmPro) were used in this study for the entire period of CATS operation on the ISS (~Feb. 2015–Oct. 2017). CATS L2 profile data are provided at 5 km along-track horizontal resolution and 533 vertical levels at 60 m vertical resolution and a wavelength of 1064 nm. CATS also provides data at 532 nm, but due to a laser-stabilization issue, 532 nm data is not recommended for use (Yorks et al. 2016). Thus, only 1064 nm products were used in this study. CATS data are quality-assured following a manner similar to Campbell et al. (2012), which was applied to CALIOP. QA thresholds (including extinction QC flag, Feature Type Score, and uncertainty in extinction coefficient) are listed below:

(a) Extinction_QC_Flag_1064_Fore_FOV is equal to 0

(b) Feature_Type_Fore_FOV = 3 (aerosol only)

(c) -10 <= Feature_Type_Score_FOV <= -2

(d) Extinction_Coefficient_Uncertainty_1064_Fore_FOV <= 10 km^{-1}

Extinction was also constrained using a threshold as provided in the CATS data catalog (Extincton_Coefficient_1064_Fore_FOV <= 1.25 km^{-1}), similar to several previous studies (Redemann et al., 2012; Toth et al., 2016). Only profiles with extinction coefficient values less than 1.25 km^{-1} are included in this study. Small negative extinction coefficient values, however, are included in aerosol profile related analysis, to reduce potential high biases in computed mean profiles. Note that a similar approach has also be conducted in deriving passive-based AOD climatology (e.g. Remer et al., 2005). For this study, both the Aerosol_Optical_Depth_1064_Fore_FOV and Extinction_Coefficient_1064_Fore_FOV datasets were used to provide AOD and 1064 nm extinction profiles (hereafter the term "extinction" will refer to 1064 nm unless explicitly stated otherwise), respectively.

2.2 CALIOP

NASA's CALIOP is an elastic backscatter lidar that operates at both 532 nm and 1064 nm wavelengths (Winker et al., 2009). Being a part of the A-Train constellation (Stephens et al., 2002), CALIOP provides both day- and night-time observations of Earth's atmospheric system, at a sun-synchronous orbit, with a laser spot size of around 70 m and a temporal resolution of ~16 days (Winker et al., 2009). For this study, CALIOP Level 2.0 Version 4.1 5 km Aerosol Profile products (L2_05kmAProf) are used for inter-comparing to CATS retrieved AODs and aerosol vertical distributions.

L2_05kmAProf data are available at 5 km horizontal resolution along-track and include aerosol retrievals at both 532 nm and 1064 nm wavelengths. The vertical resolution is 60 m near-surface, degrading to 180 m above 20.2 km in MSL altitude. As only 1064 nm CATS data are used in this study as mentioned above, likewise only those CALIOP parameters relating to 1064 nm are used in this study (Vaughan et al., 2018; Omar et al., 2013). Note that as suggested by Rajapakshe et al. (2017), lower signal-to-noise ratio (SNR) and higher minimum detectable backscatter are found for the CALIOP 1064 nm data in-comparing with the CALIOP 532 nm data. Also, the CALIOP aerosol layers are detected at 532 nm and the 1064 nm extinction is only computed for the bins within these layers. This may introduce a bias for aerosol above cloud studies. In this study, Extinction_Coefficient_1064 and Column_Optical_Depth_Tropospheric_Aerosols_1064 are used for CALIOP extinction and AOD retrievals, respectively (Vaughan et al., 2018; Omar et al., 2013). As with the CATS data, CALIOP data are quality-assured following the quality assurance steps as mentioned in a few previous studies (e.g. Campbell et al., 2012; Toth et al., 2016; 2018). These QA thresholds are listed below:

(a) Extinction_QC_Flag_1064 is equal to 0,1,2,16, or 18

(b) Atmospheric_Volume_Description = 3 or 4 (aerosol only)

(c) -100 <= CAD_Score <= -20

(d) Extinction_Coefficient_Uncertainty_1064 <= 10 km^{-1}

Furthermore, as in Campbell et al. (2012), only those profiles with AOD > 0 were retained in order to avoid profiles composed of only retrieval fill values. Extinction was also constrained to the nominal range provided in the CALIOP data catalog (Extinction_1064 <= 1.25 km -1), similar to our QA procedure for CATS as described above.

2.3 MODIS Collection 6.1 Dark Target product

Moderate Resolution Imaging Spectroradiometer (MODIS) Aqua and Terra Collection 6.1 Dark Target over-ocean AOD data (Levy et al., 2013) were used for comparison to CATS AOD.

The data field of "Effective_Optical_Depth_Best_Ocean" were used and only those data flagged as "good" or "very good" by the Quality_Assurance_Ocean runtime QA flags are selected for this study, similar to Toth et al. (2018). Because MODIS does not provide AOD in the 1064 nm wavelength, AOD retrievals from 860 and 1240 nm spectral channels are used to logarithmically interpolate AODs at 1064 nm. Here we assume the angstrom exponent value, computed using instantaneous AOD retrievals at the 860 and 1240 nm, remains the same for the 860 to 1064 nm wavelength range, similar to what has been suggested by Shi et al., (2011; 2013). Only totally cloud free (or cloud fraction equal to zero) retrievals, as indicated by the Cloud_Fraction_Land_Ocean parameter are used.

2.4 AERONET

By measuring direct and diffuse solar energy, AERONET observations are used for retrieving AOD and other ancillary aerosol properties such as size distributions (Holben et al., 1998). AERONET data are considered as the ground truth for evaluating CATS retrievals in this study. Only cloud screened and quality assured version 3 level 2 AERONET data at the 1020 nm spectrum are selected and are used for inter-comparing with CATS AOD retrievals at the 1064 nm wavelength. AERONET does not have specific guidance on error in the 1020 nm channel, as it is known to have some thermal sensitivities. However they do report significantly more confidence in version 3 of the data, which has temperature correction (Giles et al., 2018). Error models are ongoing, and for this study we assume double the RMSE, or +/-0.03.

3.0 Results & Discussion

3.1 Inter-comparison of CATS data with AERONET, MODIS and CALIOP data

Note that most evaluation efforts for passive- and active-based AOD retrievals are focused on the visible spectrum and the performance of AOD retrievals at the 1064 nm channel is less explored. Thus, in this sub-section, the performance of over land and over ocean CATS AOD retrievals are compared against AERONET and C6.1 over ocean MODIS DT aerosol products. In AOD related studies, ~~CAT~~ and CALIOP reported AOD values are used. However, ~~although not derived in this study,~~ only AOD values with corresponding aerosol vertical extinction that meet the QA criteria as mentioned in Sections 2.1 and 2.2 were used. CATS derived aerosol extinction vertical distributions are also ~~cross-~~compared against collocated CALIOP aerosol extinction vertical distributions.

3.1.1 CATS-AERONET

As the initial check, CATS data from Feb. 2015-Oct. 2017 are spatially (within 0.4 degree Latitude and Longitude) and temporally (±30minutes) collocated against ground-based AERONET data. Note that one AERONET measurement may be associated with several CATS retrievals in both space and time, and vice versa. Thus, both CATS and AERONET data are further averaged spatially and temporally, which results in only one pair of collocated and averaged CATS and AERONET data for a given collocated incident. Also, only data pairs with AOD larger than 0 from both instruments are used for the analysis. This step is necessary to exclude CATS profiles with all retrieval fill values as discussed in Section 2 (Toth et al., 2018). Such profiles containing all retrieval fill values were found to make up approximately 5.4% of all CATS profiles in the dataset. Note that the CATS-AERONET comparisons are for daytime only, and higher uncertainties are expected for CATS daytime than night AODs.

As shown in Figure 1a, without quality-assurance procedures, high spikes in CATS AOD of above 1 (1064 nm) can be found for collocated AERONET data with AOD less than 0.3 (1020 nm). Those high spikes in CATS AOD may due to cloud contamination in the V2-01 CATS daytime data, which will be improved in the upcoming CATS V3-00 data products. Upon completion of the QA steps as outlined in Section 2.1, a reasonable agreement is found between quality-assured CATS (1064 nm) vs. AERONET (1020 nm) AODs with a correlation of 0.64 (Figure 1b). Comparing Figure 1a with 1b, with the loss of only ~10% of collocated pairs due to the QA procedures, we have observed an overall improvement in correlation between CATS and AERONET AOD from 0.17 to 0.64. Note that similar results are found in comparisons between collocated CATS and MODIS/CALIOP data without the use of QA procedures on CATS data. Thus, only QAed CATS data are used hereafter. Still, this exercise highlights the need for careful quality checks of the CATS data before applying the CATS data for advanced applications to overcome cloud-aerosol discrimination uncertainties.

3.1.2 CATS-MODIS

To examine over ocean performance, column integrated CATS AODs are inter-compared with collocated Terra and Aqua C6.1 MODIS DT over ocean AOD, interpolated to 1064 nm. Over ocean C6.1 MODIS DT data are selected due to the fact that higher accuracies are reported for over ocean versus over land MODIS DT AOD retrievals (Levy et al., 2013). In addition, comparing with over land MODIS DT data, which provides AOD retrievals at three discrete wavelengths (0.46, 0.55 and 0.65 µm), over water AOD retrievals are available from 7 wavelengths including the 0.87 and 1.24 µm spectral channels, allowing a comparison with CATS AOD at the same wavelength upon interpolation.

MODIS and CATS AOT retrievals are collocated for the study period of Feb. 2015-Oct. 2017 (Figure 2). Pairs of CATS and MODIS data were first selected for both retrievals that fall within ±30 minutes and 0.4 degrees latitude and longitude of each other. Then, similar to the AERONET and CATS collocation procedures, collocated pairs were further averaged to construct one pair of collocated MODIS and CATS data for a given collocation incident. Shown in Figure 2a, a correlation of 0.71 is found between collocated over water Terra MODIS C6.1 DT and CATS AODs with a slope of 0.78. Similar results are found for the comparisons between over water Aqua MODIS and CATS AODs with a correlation of 0.75 and a slope of 0.79.

3.1.3 CATS-CALIOP AOD

In the previous two sections, AODs from CATS are inter-compared with retrievals from passive-based sensors such as MODIS and AERONET. In this section, AOD data from CALIOP, which is an active~~-based~~ sensor, are evaluated against AOD retrievals from CATS. Again, for each collocation incident, pairs of CALIOP and CATS data are selected in which both retrievals fall within ±30 minutes temporally and 0.4 degrees latitude and longitude spatially. There could be multiple CATS retrievals corresponding to one CALIOP data point, and vice versa. Thus, the collocated pairs are further averaged in such a way that only one pair of collocated CATS and CALIOP data is derived for each collocation incident. Note that as suggested by Omar et al., (2013), the choices of spatial and temporal collocation windows have an effect on collocation results. However, we consider this as a topic beyond the scope of this study.

Figure 3a shows the comparison of CATS and CALIOP AODs for all collocated pairs including both day- and night-time. A reasonable correlation of 0.7, with a slope of 0.69, is found for a total of 2681 collocated data pairs. Further breaking down the comparison into day and night cases, a much better agreement is found between the two datasets during nighttime with a correlation of 0.84 and 0.81 for over-ocean and over-land cases respectively. In comparison, a lower correlation of 0.62, with a slope of 0.44, is found between the two datasets, using over land daytime data only, for a total of 171 collocated pairs. Correspondingly, a lower correlation of 0.52, with a slope of 0.63, is found between the two datasets, using over ocean daytime data only, for a total of 1207 collocated pairs. This result is not surprising as daytime data from both CALIOP and CATS are ~~expected to be~~ nosier due to solar contamination (e.g. Omar et al., 2013; Toth et al., 2016).

Still, larger discrepancies between CATS and CALIOP AODs during daytime indicate that both sensors are ~~more~~ susceptible to solar contamination. To overcome solar contamination and more accurately detect aerosol layers, CALIOP and CATS data products are averaged up to 80 km and 60 km, respectively. Noel et al. (2018) found that clouds screened using the feature type score were accurately detected by CATS data products throughout the diurnal envelope of solar angles. To ensure the solar contamination does not introduce a diurnal bias in aerosol detection or products, CATS AODs are further evaluated as a function of local time. For each CATS observation of a given location and UTC time, the associated local time is computed by adding (subtracting) the UTC time by 1 hour per 15° Longitude away from the Prime Meridian in the east (west) direction. Figure 4a shows the CATS AOD versus local time for both global land and oceans. While noisy in data, an averaged AOD peak is found around local noon that is about 0.02-0.03 higher than both sunrise and sunset times. Still, for high AOD cases, no significant solar noon peak is found. Also, no major deviations in AODs are found during either sunrise or sunset time, although we speculate that larger uncertainties in CATS AODs and extinctions may be present around day and night terminators. Figure 4b shows a similar plot as Figure 4a, but with the region restricted to 25°S-52°S. Here, we want to investigate the variations in CATS AODs as a function of local time, over relatively aerosol free oceans. We picked 25°S as the cutoff line as CATS data only available to 51.6°S (limited to the ISS inclination angle) and thus, this threshold is used to ensure enough data samples in the analysis, although some land regions are also included. As indicated in Figure 4b, a clear diurnal variation is found, with the mean AOD values of 0.07-0.08 found between late morning and early afternoon and smaller AOD values of 0.06 found for both sunrise and sunset times. Also, no significant deviations in pattern are found for both sunrise and sunset time, plausibly indicating that solar contamination, as speculated, may not be as significant. It is, however, unclear if the 0.02 AOD difference between local noon and sunrise and sunset times is introduced by retrieval bias or indeed a physical existence.

To further explore the 0.02 difference, Figure 4c shows the difference between AERONET (1020 nm) and CATS (1064 nm) AOD (ΔAOD) as a function of local time, again, although data are rather noisy, no major pattern is found near sunrise or sunset times, again, further indicating that solar contamination during dawn or dusk times, may have a less severe impact to CATS AOD retrievals from a long term mean perspective.

In summary, Sections 3.1.1-3.1.3 suggest that with careful QA procedures, AOD retrievals from CATS are comparable to those from other existing sensors such as AERONET, MODIS, and CALIOP at the same local times.

3.1.4 CATS-CALIOP Vertical Extinction Profiles

One advantage of CATS is its ability to retrieve both column-integrated AOD and vertical distributions of aerosol extinction. Therefore, in this section, extinction profiles from CATS are compared with that from CALIOP. Again, similar to the Section 3.1.3, collocated profiles for CATS and CALIOP are first found for both retrievals that are close in space and time (within ±30 minutes and 0.4 degrees latitude and longitude). However, different from Section 3.1.3, only one pair of collocated CATS and CALIOP profiles, which has the closest Euclidian distance on the earth's surface, is retained for each collocated incident.

The CATS cloud-aerosol discrimination (CAD) algorithm is a multidimensional probability density function (PDF) technique that is based on the CALIPSO algorithm (Liu et al. 2009). The PDFs were developed based on Cloud Physics Lidar (CPL) measurements obtained during over 11 field campaigns and 10 years. Figure 5 shows that CATS V2-01 aerosol extinction agrees very well with CALIOP for nighttime (Figure 5c) and over land (Figure 5e). However, CATS overestimates aerosol extinction around 1 km compared to CALIOP during daytime (Figure 5b) and over ocean (Figure 5d). This can also be seen on a plot of the difference between CATS and CALIOP 1064 nm extinction for all collocated profiles, included in Appendix A, where there is an overall positive difference around 1 km. Based on statistical comparisons of CATS L2O V2-01 cloud and aerosol detection frequencies with CALIOP, it was determined that, during daytime over ocean, depolarizing liquid water clouds in the lower troposphere are sometimes classified as lofted dust mixture or smoke aerosols in the CATS V2-01 data products. This is primarily a result of enhanced depolarization ratios within liquid water clouds due to multiple scattering (which is not represented in the CPL measurements used for the PDFs). To overcome this issue, the CATS V3-00 CAD algorithm uses horizontal persistence tests and additional tests using variables such as the perpendicular ATB, to better differentiate clouds and aerosols. More details will be provided in an upcoming paper (Yorks et al., in prep). Since the CATS V3-00 data has not been released yet, we will focus our discussion of aerosol diurnal variability on regions primarily over land.

In addition, due to the precessing orbit of the ISS, the CATS sampling is irregular and very different compared to the sun-synchronous orbits of the A-Train sensors. These orbital differences between CATS and CALIOP make comparing the data from these two sensors challenging since they are fundamentally observing different locations of the Earth at different times. Thus, we shouldn't expect the extinction profiles and AOD from these two sensors to completely agree. Additionally, there are other algorithm and instrument differences that can lead to differences in extinction coefficients and AOD. Over land where dust is the dominant aerosol type, differences in lidar ratios between the two retrieval algorithms (CATS uses 40 sr while CALIOP uses 44 sr), can cause CATS extinction coefficients that are up to 10% lower than CALIOP, potentially explaining the higher CALIOP extinction values in Figure 5e. Over ocean, especially during daytime, differences in CATS and CALIOP lidar ratios for marine and smoke aerosols, as well as issues with CATS cloud-aerosol discrimination in V2-01 for daytime observations, can cause CATS extinction coefficients that are as much as 25% higher than CALIOP (Figure 5b and 5d). Yorks et al. (2019) shows examples of these daytime cloud-aerosol discrimination issues in V2-01 data, which have been improved for CATS V3-00 data. A brief analysis using 3 months of CATS V3-00 data showed improvement in agreement for AOD, but some differences were still evident in the extinction vertical profiles. These remaining differences, as well as the differences observed in nighttime only profiles (Figure 5c) are likely attributed to differences in CATS and CALIOP 1064 nm backscatter calibration. Pauly et al. (2019) reports that CATS attenuated total backscatter is about ~~18% higher than CALIOP due to calibration uncertainties for both sensors~~.

CATS also has a stronger extinction when compared to CALIOP in the lowest 2 km, which may be due to differences in cloud screening. Vertical profiles of collocated CATS and CALIOP extinction for daytime only profiles and nighttime only profiles are shown in Figure 5b and 5c, respectively. Compared to a total collocated pair count of 2681 in the overall profile data, day and night profiles have 1342 and 1339 collocated pairs, respectively. Again, the shapes of the CATS and the CALIOP nm extinction vertical profile are very similar for all three cases, despite the above mentioned offsets in altitude. Figure 5d and 5e show the mean of those extinction profiles which occurred over-water and over-land, as defined by the CATS surface type flag. Again in both cases CATS and CALIOP have very similar shapes in their vertical extinction profiles. The vertical structure of over-water extinction is also very similar to that of all profiles, day, and night, which is perhaps not surprising as water profiles made up 2111 of 2681 (~79%) collocated pairs. The vertical structure of over-land is more different than the other groups, as the extinction is higher throughout a larger depth of the atmosphere, tapering off much more slowly from the surface. Furthermore, the extinction from CATS is actually lower than CALIOP for over-land profiles, unlike all other categories.

3.2 Diurnal Cycle of AODs and Aerosol Vertical Distributions

Using the QAed CATS data, seasonal variations as well as diurnal variations in CATS AODs are derived in this section. Diurnal variations in the vertical distributions of CATS aerosol extinction are also examined at both global and regional scales.

3.2.1 Seasonal and Diurnal Variation of AOD

Figures 6a-b show the spatial distributions of CATS AODs at the 1064 nm spectral channel for boreal winter-spring (Dec.-May, DJFMAM) and boreal summer-fall (June-Nov, JJASON) seasons, for the period of Feb. 2015-Oct. 2017. To construct Figures 6a and 6b, quality-assured CATS AODs are first binned on a 5 degree by 5 degree grid over the globe for the above mentioned two bi-seasons. For each 5×5° (Latitude/Longitude) bin, for a given season, CATS AODs are averaged on a pass-basis first, and then further averaged seasonally to represent AOD value of the given bin.

In DJFMAM season, significant aerosol features are found over North Africa, Mid-East, India and Eastern China. For the JJASON season, besides the above mentioned regions, aerosol plumes are also observable over Southern Africa, related to summer biomass burning of the region (e.g. Eck et al., 2013). The seasonal-based spatial distributions of AODs from CATS, although reported at the 1064 nm channel which is different from the 550 nm channel that is conventionally used, are similar to some published results (e.g. Lynch et al., 2016).

For comparison purposes, Figures 6c-6d shows similar plots as Figures 6a-6b, but with the use of CALIOP AOD at the 1064 nm ~~spectral~~ channel. Note that those are climatological means rather than pairwise comparisons. While patterns are similar in general, at regions with peak AODs of 0.4 or above for CALIOP, such as North Africa for the DJFMAM season and North Africa, Middle-East and India for the JJASON, much lower AODs are found for CATS. In some other regions, such as over South Africa and upper-portion of Middle-East for the JJASON season, however, higher CATS AOD values are observed. A table of mean AOD across each of these regions as well as over the globe (within the latitude range where CATS has data) has been included for reference (Table 2). Figures 6e and 6f show the similar spatial plots as Figures 6a and 6b but with the use of Aqua MODIS AODs from the DT products. For the Aqua MODIS DT products, aerosol retrievals at the short-wave Infra-red channels are only available over oceans, and thus Figures 6e-6f show only over ocean retrievals. Again, while general AOD ~~patters~~ look similar, discrepancies are also visible, such as over the coast of south east Africa for the JJASON season. Those discrepancies may result from biases in each product, but it is also possibly due to the differences in satellite overpass times, as CALIOP provides early morning and afternoon over passes, and Aqua MODIS has an over pass time after local noon, while CATS is able to report atmospheric aerosol distributions at multiple times during a day. It is also possibly due to aerosol above cloud related issues as reported by Rajapakshe et al. (2017), as explained in Section 2.2.

Similar to Figures 6a and 6b, Figures 7a and 7b show the spatial distribution of CATS AODs, but for CATS extinction values that are below 1 km Above Ground Level (AGL) only, for the DJFMAM and JJASON seasons respectively. Figure 7c and 7d (7e and 7f) show the CATS mean AOD plots for extinction values from 1-2 km AGL (> 2 km AGL). For the DJFMAM season, elevated aerosol plumes with altitude above 2 km AGL are found over the North coast of Africa. For the JJASON season, elevated dust plumes (> 2 km AGL) are found over North Africa and the Middle-East regions, while elevated smoke plumes are found over the west coast of South Africa where above cloud smoke plumes are often observed during the Northern hemispheric summer season (e.g. Alfaro-Contreras et al., 2016).

CATS has a non-sun-synchronized orbit, which enables measurements at near all solar angles. Thus, we also constructed 5×5° (Latitude/Longitude) gridded seasonal averages (for DJFMAM and JJASON seasons) of CATS AODs at 0, 6, 12 and 18 UTC that represent 4 distinct times in a full diurnal cycle, as shown in Figure 8. To construct the seasonal averages, observations within ±3 hours of a given UTC time as mentioned above are averaged to represent AODs for the given UTC time. On a global average, the mean AODs are 0.090, 0.090, 0.090 and 0.091 for 0, 6, 12 and 18 UTC respectively for the JJASON season and are 0.101, 0.100, 0.097 and 0.097 for the DJFMAM season. Thus, no significant diurnal variations are found on a global scale, as global means are dominated by background aerosols that have weak diurnal variations in measured absolute AOD values.

Still, strong diurnal variations with the maximum averaged diurnal AOD changes of above 0.15 can be observed for regions with significant aerosol events such as Northern Africa and India for the DJFMAM season and Northern Africa, Southern Africa, Mid-East and India for the JJASON season, as illustrated in Figure 9. Note that Fig. 9a (9b) shows the maximum minus minimum seasonal mean AODs for the four difference times as shown in Figs. 8a,c,e,g (8b,d,f,h). Interestingly but not unexpectedly, regions with maximum diurnal variations match well with locations of heavy aerosol plumes as shown in Figures 6 and 8.

3.2.2 Diurnal variations of Aerosol Extinction on a Global Scale (both at UTC and local time)

Using quality-assured CATS derived aerosol vertical distributions, mean global CATS extinction vertical profiles are also generated as shown in Figure 10. Similar to steps as described in ~~the~~ section 3.2.1, CATS extinction profiles are binned into 00, 06, 12, and 18 UTC times based on the closest match in time for the JJASON and DJFMAM seasons. Figure 10a (10d) shows the daily averaged CATS extinction profiles in a black line, and 00, 06, 12 and 18 UTC averaged in blue, green, yellow and red lines respectively, for the DJFMAM (JJASON) season. CATS extinction profiles for the daily average as well averages for the four selected times are similar, suggesting that minor temporal variations in CATS extinctions can be expected for global averages.

Those global averages are dominated by CATS profiles from global oceans (Figure 10b and 10e), which also have small diurnal variations, as ~70% of the globe is covered by water. In comparison, noticeable diurnal changes in aerosol vertical distributions are found over land as shown in Figure 10c and 10f. For the DJFMAM season, at the 1 km altitude, the minimum and maximum aerosol extinctions are at 12 and 18 UTC respectively. Similarly, the minimum and maximum aerosol extinctions are at 18 and 6 UTC at the altitude of 400 m. For the JJASON season, the minimum aerosol extinction values are found at 12 UTC for the whole 0-2 km column, while the maximum aerosol extinction values are at 18UTC for 1.5 km and 0UTC for the 300-400 m altitude. Still, it should be noted that aerosol concentrations may be a function of local time, yet for a given UTC time, local times will vary by region. Also, due to solar contamination, nighttime retrievals from CATS are significantly and demonstrably less noisy than daytime retrievals, and this difference in sensor sensitivity between day and night may further affect the derived diurnal variations in CATS AOD and aerosol vertical profiles as shown in Figure 3 for individual retrievals. Still, no apparent solar pattern is detectable from Figure 8, and only minor diurnal variations are found for Figure 10a and 10d, which indicate that such a solar contamination may introduce noise but not bias to daytime aerosol retrievals, from a global mean perspective.

If we examine the mean global CATS extinction vertical profiles with respect to local time as shown in Figure 11, however, some distinct features appear. For example, Figure 11a and 11d suggests that on global average, the minimum and maximum aerosol extinction below 1 km is found for 6:00 pm and 12:00 pm local time, respectively for both JJASON and DJFMAM seasons. Similar patterns are also observed for over global oceans. However, for over land cases, for both seasons, peak in aerosol extinction is found at the 500-1000 m layer for local noon, which is ~20-30% higher than daily mean values. This may indicate stronger solar heating at the surface and hence stronger near surface convection at local noon that brings near surface aerosol particles to a higher altitude.

3.2.3 Diurnal variations of Aerosol Extinction on a Regional Scale (at local time)

In this section, the diurnal variations of aerosol vertical distributions are studied as a function of local solar time for selected regions with high mean AODs as highlighted in Figure 6. We picked local solar time here as for those regional analyses, near 1 to 1 transformation can be achieved between UTC and local solar time. Also, as learned from the previous section, aerosol features are likely to have a local time dependency. A total of four regions, including Africa-north, Middle East, India and Northeast China, which show significant seasonal mean AODs in Figure 6, are selected for the DJFMAM season (Figure 12). For the JJASON season (Figure 13), in addition to the above mentioned 4 regions, the Africa-south region is also included due to biomass burning in the region during the Northern Hemisphere summer time. The Latitude/Longitude boundary of each selected region is described in Table 1. Regional-based analyses are also conducted for 4 (5) selected regions for the DJFMAM (JJASON) season at four local times: 0:00 am, 6:00 am, 12:00 pm and 6:00 pm, using quality assured CATS profiles. Generally, the maximum diurnal change in aerosol extinction is found at the altitude of below 1 km for all regions as well for both seasons. Also, larger diurnal variations in vertical distributions of aerosol extinction are found for the JJASON season, in-comparing with the DJFMAM season, while regional-based differences are apparent.

For the Africa-north region, dominant aerosol types are dust and smoke aerosol for the DJFMAM season, and is dust for the JJASON season (e.g. Remer et al., 2008). Interestingly, the maximum aerosol extinction below 500m is found at 6:00 am for the DJFMAM season. While for the JJASON season, the maximum aerosol extinctions are found at 6:00 am for the whole 0-2 km column, with a significant ~20% higher aerosol extinction from either daily mean or vertical profiles from 0:00 am, 12:00 pm and 6:00 pm. Note that 6:00 am in the Africa-north region corresponds to early morning, which has been identified in several studies (Fiedler et al., 2013;

Ryder et al. 2015) as the time of day when nocturnal low-level jet breakdown causes large amounts of dust emission in this region. Thus, we suspect that this large 6:00 am peak in maximum aerosol extinctions may be the signal resulting from the low-level jet ejection mechanism captured on a regional scale. As the day progresses into the afternoon and early evening, we find the aerosol heights shifting upwards, likely related to the boundary layer's mixed layer development.

For the Middle East region, for the JJASON season, a daily maximum in aerosol extinction of ~0.13 km^{-1} is found at local morning or early morning (0:00 am and 6:00 am) , with a daily minimum of ~0.09 km^{-1} found at local noon (12:00 pm), for the peak aerosol extinction layer that has a daily mean aerosol extinction of ~~0.11 km^{-1}. This translates to a ~±20% daily variation for aerosol extinction for the peak aerosol extinction layer. Much smaller daily variation in aerosol extinction, however, is found for the same region for the DJFMAM season.

For the India region, for the JJASON season, a large peak in aerosol extinction of up to 20% higher than daily mean is found at 6:00 am below 1 km. The minimum aerosol extinction is found at 0:00 am for the layer of ~400-1000 m, and is overall ~10% lower than the daily means. The minimum aerosol extinction is found at 6:00 pm for the layer below 400 m. For the DJFMAM season, minimum aerosol extinctions are found at 12:00 pm for near the whole 0-2 km column, while for the layer below 500 m, the maximum aerosol extinction values are found at early morning (0:00 am and 6:00 am). This is consistent with the diurnal formation of significant haze.

For the Northeast China region, less diurnal variation is found for the DJFMAM season. Yet, a significant peak found at 1km for local noon (12:00 pm) for the JJASON season, which is ~30% higher than daily averages for the JJASON season. The reason for this elevated peak at regional local noon, however, is not known, although it may relate to the peak in surface Particulate Matter concentrations. Lastly, for the Africa-south region, biomass burning aerosols are prevalent during the summer time and thus only the JJASON season is analyzed. As shown in 13b, below 500m in altitude, lower extinction values are found for local afternoon (12:00 pm and 6:00 pm) and higher extinction values are found for local morning or early morning (0:00 and 6:00 am). Still, the diurnal variation in aerosol vertical distribution is rather marginally for the region.

4.0 Conclusions

Using CALIOP, MODIS and AERONET data, we evaluated CATS derived AODs as well as vertical distributions of aerosol extinctions for the study period of for Feb. 2015 – Oct. 2017. CATS data (at 1064 nm) are further used to study variations in AODs and aerosol vertical distributions diurnally. We found:

(1) Quality assurance steps are critical for applying CATS data in aerosol related applications. With a 10% data loss due to QA steps, an improvement in correlation from 0.17 to 0.64 is found for the collocated CATS and AERONET AOD comparisons. Using quality assured CATS data, reasonable agreements are found between CATS derived AODs and AODs from CALIOP, Aqua MODIS DT and Terra MODIS DT at the same local times, with correlations of 0.70, 0.75 and 0.71 respectively.

(2) While the averaged vertical distributions from CATS compare reasonably well with that from CALIOP, differences in peak extinction altitudes are present. This may due to contamination of daytime aerosol detections over ocean by marine boundary layer clouds in the CATS V2-01 data products, which will hopefully be resolved in the future CATS V3-00 data.

(3) From the global mean perspective, minor changes are found for AODs at four selected times, namely 00, 06, 12 and 18 UTC. Yet noticeable diurnal variations in AODs of

above 0.15 (at 1064 nm) are found for regions with extensive aerosol events, such as over North Africa, and India for the DJFMAM season, and over North and South of Africa, India and Middle East for the JJASON season.

(4) From the global mean perspective, changes are less noticeable for the averaged aerosol extinction profiles at 00, 06, 12 and 18 UTC. Yet, if the study is repeated with respect to local time, a peak in aerosol extinction is found for local noon and the minimum value in aerosol extinction is found at 6:00 pm local time for both JJASON and DJFMAM seasons. In particular, for over land cases, in both seasons, a lifted aerosol plume at 500-1000 m altitude (with the peak aerosol extinction that is ~20-30% higher that daily averages) is found at local noon, which may indicate the impact of strong surface solar heating as well as stronger near surface convection on aerosol vertical distributions.

(5) Larger diurnal variations are found at regions with heavy aerosol plumes such as North and South (summer season only) of Africa, Middle East, India and Eastern China. In particular, aerosol extinctions from 6:00 am over North Africa are ~20% higher than daily means as well other three times for the 0-2 km column for the JJASON season. We suspect this may be related to increase in dust concentrations due to breakdown of low level jets at early morning time for the region.

(6) Still, readers shall be aware that AOD retrievals at the 1064 nm are less sensitive to fine mode aerosols such as smoke and pollutant aerosols, compared to coarse mode aerosols such as dust aerosols. Thus, an investigation of diurnal variations of aerosol properties at the visible channel may be also needed for a future study.

This paper suggests that strong regional diurnal variations exist for both AOD and aerosol extinction profiles. Still, at present these conclusions are tentative, and will remain so until a comprehensive analysis of the CATS calibration accuracy and stability is completed. These results demonstrate the need for global aerosol measurements throughout the entire diurnal cycle to improve visibility and particulate matter forecasts as well as studies focused on aerosol climate applications.

Author Contribution:

Authors J. Zhang, J. S. Reid and L. Lee designed the study. L. lee worked on data processing for the project. J. E. Yorks guided L. lee on data processing. The manuscript was written with inputs from all coauthors.

Acknowledgments:

We acknowledge the support of ONR grant (N00014-16-1-2040) and NASA grant (NNX17AG52G) for this study. L. Lee is also partially supported by the NASA NESSF fellowship grant (NNX16A066H). J. S Reid’s participation was supported by the Office of Naval Research Code 322 and 33. We thank the NASA AERONET team for the AERONET data used in this study.

References:

Aerosol Product Application Team of the AWG Aerosols/Air Quality/Atmospheric Chemistry Team: GOES-R Advanced Baseline Imager (ABI) algorithm theoretical basis document for suspended matter/aerosol optical depth and aerosol size parameter, NOAA/NESDIS/STAR July 2012, https://www.star.nesdis.noaa.gov/goesr/docs/ATBD/AOD.pdf (last accessed on Nov. 17, 2018).

Alfaro-Contreras, R., Zhang, J., Campbell, J. R., and Reid, J. S.: Investigating the frequency and trends in global above-cloud aerosol characteristics with CALIOP and OMI, Atmos. Chem. Phys., 16, 47-69, doi:10.5194/acp-16-47-2016, 2016.

Campbell, J. R., Tackett, J. L., Reid, J. S., Zhang, J., Curtis, C. A., Hyer, E. J., Sessions, W. R., Westphal, D. L., Prospero, J. M., Welton, E. J., Omar, A. H., Vaughan, M. A., and Winker, D. M.: Evaluating nighttime CALIOP 0.532 μm aerosol optical depth and extinction coefficient retrievals, Atmos. Meas. Tech., 5, 2143-2160, https://doi.org/10.5194/amt-5-2143-2012, 2012.

CATS Algorithm Theoretical Basis Document: https://cats.gsfc.nasa.gov/media/docs/CATS_ATBD_V1-02.pdf, 2016; accessed on March 28, 2019.

Christopher, S. A. and Zhang, J.: Daytime variation of shortwave direct radiative forcing of biomass burning aerosols from GOES 8 imager, J. Atmos. Sci., 59, 681–691, 2002.

Eck, T .F., Holben, B. N., Reid, J. S., Mukelabai, M. M., Piketh, S. J., Torres, O., Jethva, H. T., Hyer, E. J., Ward, D. E., Dubovik, O., and Sinyuk, A.: A seasonal trend of single scattering albedo in southern African biomass-burning particles: Implications for satellite products and estimates of emissions for the world's largest biomass-burning source, J. Geophys. Res.-Atmos., 118, 6414–6432, 2013.

Fiedler, S., Schepanski, K., Heinold, B., Knippertz, P., and Tegen, I.: Climatology of nocturnal low-level jets over North Africa and implications for modeling mineral dust emission, J. Geophys. Res. Atmos., 118, 6100–6121, doi: 10.1002/jgrd.50394, 2013.

Giglio, L., Kendall, J.D., Mack, R.: A multi-year active fire dataset for the tropics derived from the TRMM VIRS,. International Journal of Remote Sensing 24, 4505-4525, 2003.

Giles, D. M., Sinyuk, A., Sorokin, M. S., Schafer, J. S., Smirnov, A., Slutsker, I., Eck, T. F., Holben, B. N., Lewis, J., Campbell, J., Welton, E. J., Korkin, S., and Lyapustin, A.: Advancements in the Aerosol Robotic Network (AERONET) Version 3 Database – Automated Near Real-Time Quality Control Algorithm with Improved Cloud Screening for Sun Photometer Aerosol Optical Depth (AOD) Measurements, Atmos. Meas. Tech. Discuss., https://doi.org/10.5194/amt-2018-272, in review, 2018.

Heinold, B., Knippertz, P., Marsham, J. H., Fiedler, S., Dixon, N. S., Schepanski, K., Laurent, B., and Tegen, I.: The role of deep convection and nocturnal low-level jets for dust emission in summertime West Africa: Estimates from convection-permitting simulations, J. Geophys. Res. Atmos., 118, 4385–4400, doi:10.1002/jgrd.50402, 2013.

Holben, B. N., and coauthors: AERONET—A Federated Instrument Network and Data Archive for Aerosol Characterization. Remote Sensing of Environment, 66(1), 1–16. https://doi.org/10.1016/S0034-4257(98)00031-5, 1998.

Hyer, E. J., Reid, J. S., Prins, E. M., Hoffman, J. P., Schmidt, C. C., Miettinen, J. I., and Giglio, L.: Different views of fire activity over Indonesia and Malaysia from polar and geostationary satellite observations, *Atmos. Res.*, 122, 504-519, 2013.

Kaku K. C., Reid, J. S., Hand, J. L., Edgerton, E. S., Holben, B. N., Zhang, J., and Holz, R. E.: Assessing the challenges of surface-level aerosol mass estimates from remote sensing during the SEAC4RS campaign: Baseline surface observations and remote sensing in the Southeastern United States, JGR, doi: 10.1029/2017JD028074, 2018.

Levy, R. C., Mattoo, S., Munchak, L. A., Remer, L. A., Sayer, A. M., Patadia, F., and Hsu, N. C.: The Collection 6 MODIS aerosol products over land and ocean. Atmos. Meas. Tech., 6(11), 2989–3034. https://doi.org/10.5194/amt-6-2989-2013, 2013.

Liu, Z., and coauthors: The CALIPSO Lidar Cloud and Aerosol Discrimination: Version 2 Algorithm and Initial Assessment of Performance, *J. Atmos. Oceanic Technol.*, 26, 1198–1213, 2009.

Lynch, P., Reid, J. S., Westphal, D. L., Zhang, J., Hogan, T. F., Hyer, E. J., Curtis, C. A., Hegg, D. A., Shi, Y., Campbell, J. R., Rubin, J. I., Sessions, W. R., Turk, F. J., and Walker, A. L.: An 11-year global gridded aerosol optical thickness reanalysis (v1.0) for atmospheric and climate sciences, Geosci. Model Dev., 9, 1489-1522, https://doi.org/10.5194/gmd-9-1489-2016, 2016.

Mbourou, G. N., Berand, J. J., and Nicholson, S. E.: The diurnal and seasonal cycle of wind-borne dust over Africa north of the equator, J. Appl. Meteor., 36, 868-882, 1997.

McGill, M. J., Yorks, J. E., Scott, V. S., Kupchock, A. W., and Selmer, P. A.: The Cloud-Aerosol Transport System (CATS): A technology demonstration on the International Space Station, Proc. SPIE 9612, Lidar Remote Sensing for Environmental Monitoring XV, 96120A, doi:10.1117/12.2190841, 2015.

Noel, V., Chepfer, H., Chiriaco, M., and Yorks J. E.: The diurnal cycle of cloud profiles over land and ocean between 51° S and 51° N, seen by the CATS spaceborne lidar from the

International Space Station, Atmos. Chem. Phys., 18, 9457-9473, https://doi.org/10.5194/acp-18-9457-2018, 2018.

Omar, A. H., Winker, D. M., Tackett, J. L., Giles, D. M., Kar, J., Liu, Z., Vaughan, M. A., Powell, K. A., and Trepte C. R.: CALIOP and AERONET aerosol optical depth comparisons: One size fits none, J. Geophys. Res. Atmos., 118, 4748–4766, doi: 10.1002/jgrd.50330, 2013.

Rajapakshe, C., Zhang, Z., Yorks, J. E., Yu, H., Tan, Q., Meyer, K., Platnick, S.: Seasonally Transported Aerosol Layers over Southeast Atlantic are Closer to Underlying Clouds than Previously Reported, Geophys. Res. Lett., 44, doi:10.1002/2017GL073559, 2017.

Redemann, J., Vaughan, M. A., Zhang, Q., Shinozuka, Y., Russell, P. B., Livingston, J. M., … Remer, L. A.: The comparison of MODIS-Aqua (C5) and CALIOP (V2 & V3) aerosol optical depth. Atmospheric Chemistry and Physics, 12(6), 3025–3043. https://doi.org/https://doi.org/10.5194/acp-12-3025-2012, 2012.

Reid, J.S., Eck, T. F., Christopher, S. A., Hobbs, P. V., and Holben B. R.: Use of the Angstrom exponent to estimate the variability of optical and physical properties of aging smoke particles in Brazil, J. Geophys. Res., *104*, 27,489-27,489, 1999.

Remer, L. A., and coauthors: Global aerosol climatology from the MODIS satellite sensors, J. Geophys. Res., 113, D14S07, doi: 10.1029/2007JD009661, 2008.

Remer, L.A., Y.J. Kaufman, D. Tanré, S. Mattoo, D.A. Chu, J.V. Martins, R. Li, C. Ichoku, R.C. Levy, R.G. Kleidman, T.F. Eck, E. Vermote, and B.N. Holben, The MODIS Aerosol Algorithm, Products, and Validation. J. Atmos. Sci., **62**, 947–973, https://doi.org/10.1175/JAS3385.1, 2005.

Ryder, C. L., McQuaid, J. B., Flamant, C., Rosenberg, P. D., Washington, R., Brindley, H. E., Highwood, E. J., Marsham, J. H., Parker, D. J., Todd, M. C., Banks, J. R., Brooke, J. K., Engelstaedter, S., Estelles, V., Formenti, P., Garcia-Carreras, L., Kocha, C., Marenco, F., Sodemann, H., Allen, C. J. T., Bourdon, A., Bart, M., Cavazos-Guerra, C., Chevaillier, S., Crosier, J., Darbyshire, E., Dean, A. R., Dorsey, J. R., Kent, J., O'Sullivan, D., Schepanski, K., Szpek, K., Trembath, J., and Woolley, A.: Advances in understanding mineral dust and boundary layer processes over the Sahara from Fennec aircraft observations, Atmos. Chem. Phys., 15, 8479-8520, https://doi.org/10.5194/acp-15-8479-2015, 2015.

Shi Y., Zhang, J., Reid, J. S., Hyer, E., and Hsu, N. C.: Critical evaluation of the MODIS Deep Blue aerosol optical depth product for data assimilation over North Africa, Atmos. Meas. Tech., 6, 949-969, doi:10.5194/amt-6-949-2013, 2013.

Shi Y., Zhang J., Reid J. S., Hyer E. J., Eck T. F., and Holben B. N.: A critical examination of spatial biases between MODIS and MISR aerosol products – application for potential AERONET deployment, Atmos. Meas. Tech., 4, 2823–2836, 2011.

Stephens, G. L., and coauthors: The CLOUDSAT mission and the A-TRAIN, Bulletin of the American Meteorological Society, 83(12), 1771–1790. https://doi.org/10.1175/BAMS-83-12-1771, 2002.

Tiwari, S., Srivastava, A. K., Bisht, D. S., Parmita, P., Srivastava, M. K., and Atri, S. D.: Diurnal and seasonal variaition of black carbon and PM2.5 over New Delhi, india: Influence of meteorology, Atmos. Res, 125, 50-62, doi:10.1016/j.atmos.res.2013.01.011, 2013.

Toth, T. D., Campbell, J. R., Reid, J. S., Tackett, J. L., Vaughan, M. A., Zhang, J., & Marquis, J. W.: Minimum aerosol layer detection sensitivities and their subsequent impacts on aerosol optical thickness retrievals in CALIPSO level 2 data products. Atmospheric Measurement Techniques, 11(1), 499–514. https://doi.org/https://doi.org/10.5194/amt-11-499-2018, 2018.

Toth, T. D., Zhang, J., Campbell, J. R., Reid, J. S., & Vaughan, M. A.: Temporal variability of aerosol optical thickness vertical distribution observed from CALIOP, Journal of Geophysical Research: Atmospheres, 121(15), 9117–9139. https://doi.org/10.1002/2015JD024668, 2016.

Vaughan, M., Garnier, A., Josset, D., Avery, M., Lee, K.-P., Liu, Z., Hunt, W., Pelon, J., Tackett, J., Getzewich, B., Kar, J., and Burton, S.: CALIPSO Lidar Calibration at 1064 nm: Version 4 Algorithm, in preparation, 2018.

Wang, J., Liu, X., Christopher, S. A., Reid, J. S., Reid, E. A., and Maring, H.: The effects of non-sphericity on geostationary satellite retrievals of dust aerosols, Geophys. Res. Lett., 30(24), 2293, doi:10.1029/2003GL018697, 2003.

Winker, D. M., and coauthors: Overview of the CALIPSO Mission and CALIOP Data Processing Algorithms. Journal of Atmospheric and Oceanic Technology, 26(11), 2310–2323. https://doi.org/10.1175/2009JTECHA1281.1, 2009.

Yorks, J. E., McGill, M. J., Palm, S. P., Hlavka, D. L., Selmer, P. A., Nowottnick, E., Vaughan, M. A., Rodier, S., and Hart W. D.: An Overview of the CATS Level 1 Data Products and Processing Algorithms, Geophys. Res. Let., 43, doi:10.1002/2016GL068006., 2016.

Yorks, J. E., Rodier, S.D., Nowottnick, E., Selmer, P.A., McGill, M.J., Palm, S.P., and Vaughan, M. A.: CATS Level 2 Vertical Feature Mask Algorithms and Data Products: An Overview and Initial Assessment, Atmos. Meas. Tech. Discuss., in preparation.

Yoshida M., Kikuchi, M., Nagao, T. M., Murakami, H., Nomaki, T., and Higurashi, A.: Common Retrieval of Aerosol Properties for Imaging Satellite Sensors, Journal of the Meteorological Society of Japan. Ser. II, Article ID 2018-039, [Advance publication], https://doi.org/10.2151/jmsj.2018-039, 2018.

Zhao, X. J., Zhang, X. L., Xu, X. F., Xu, J., Meng, W., and Pu, WW.: Seasonal and diurnal variation of ambient PM2.5 concentrations in urban and rural environments in Beijing, Atmos. Environ., 43, 2893-2900, doi: 10.106/j.atmosenv.2009.03.009., 2009.

Table 1. Geographic ranges, height above ground level of maximum extinction, diurnal extinction range at height of maximum extinction, and time (local) of peak extinction for the boxed red regions in Figure 6 and vertical profiles shown in Figures 12 and 13.

DJFMAM/JJASON					
Region	Latitude	Longitude	Height AGL (m) of Max. Extinction	Extinction Range (km^{-1}) at Height AGL of Max. Extinction	Time of Peak Extinction at Height AGL of Max. Extinction
India	7.5°N - 32.5°N	65°E - 85°E	180/240	0.109-0.131/0.138-0.182	6 am/6 am
Africa - North	2.5°N - 22.5°N	35°W - 20°E	420/480	0.107-0.130/0.098-0.121	12 pm/6 am
Africa - South	17.5°S - 2.5°N	0° - 30°E	/420	/0.090-0.100	/6 am
Middle East	12.5°N - 27.5°N	35°E - 50°E	240/180	0.093-0.116/0.081-0.135	6 am/0 am
China	27.5°N - 37.5°N	110°E - 120°E	240/240	0.107-0.154/0.085-0.133	6 am/6 am

Table 2. CALIOP and CATS mean aerosol optical depth for regions as highlighted in Figure 6 and globally between +/- 52° latitude.

Region	Latitude	Longitude	Mean CATS AOD (DJFMAM/JJASON)	Mean CALIOP AOD (DJFMAM/JJASON)
Global	52°S-52°N	180°W-180°E	0.09/0.10	0.09/0.09
India	7.5°N - 32.5°N	65°E - 85°E	0.22/0.26	0.22 /0.28
Africa - North	2.5°N - 22.5°N	35°W - 20°E	0.26/0.23	0.30 /0.25
Africa - South	17.5°S - 2.5°N	0° - 30°E	0.14/0.22	0.15 /0.13
Middle East	12.5°N - 27.5°N	35°E - 50°E	0.22/0.33	0. 26/0.35
China	27.5°N - 37.5°N	110°E - 120°E	0.19/0.18	0.21 /0.16

Figure Captions

Figure 1. Collocated AERONET 1020 nm AOT vs. CATS 1064 nm AOD a) without CATS QA applied, and b) with CATS QA applied.

Figure 2. Collocated MODIS C6.1 a) Terra and b) Aqua estimated 1064 nm AOD vs. CATS 1064 nm AOD with CATS QA applied.

Figure 3. Collocated CALIOP 1064 nm AOD vs. CATS 1064 nm AOD with CATS QA applied for a) both day and night, b) nighttime over-land, c) nighttime over-water, d) daytime over-land, e) daytime over-water.

Figure 4: CATS 1064 nm AOD a) as a function of local time for the globe, and b) as a function of local time for areas south of -25 degrees. The difference between CATS 1064 nm AOD and AERONET 1020 nm AOD as a function of local time is shown in c). The mean is represented by the blue line, while the median is the green line.

Figure 5. CATS and CALIOP vertical profiles of 1064 nm extinction for a) all profiles, b) daytime only, c) nighttime only, d) over-water, and e) over land.

Figure 6. Mean AOD (1064 nm) by season for a) DJFMAM CATS, b) JJASON CATS, c) DJFMAM CALIOP, d) JJASON CALIOP, e) DJFMAM MODIS Aqua, and f) JJASON MODIS Aqua. Red boxes indicate locations of regional vertical distributions in Figures 12 and 13.

Figure 7. Mean CATS AOD (1064 nm) by season for a) DJFMAM below 1 km AGL, b) JJASON below 1 km AGL, c) DJFMAM 1-2 km AGL, d) JJASON 1-2 km AGL, e) DJFMAM above 2 km AGL, and f) JJASON above 2 km AGL.

Figure 8. Seasonal Mean AOD (1064 nm) binned by every 6-hours for a) DJFMAM 0 UTC, b) JJASON 0 UTC, c) DJFMAM 6 UTC, d) JJASON 6 UTC, e) DJFMAM 12 UTC, f) JJASON 12 UTC, g) DJFMAM 18 UTC, and h) JJASON 18 UTC.

Figure 9. Maximum minus minimum mean seasonal AOD (1064 nm) for a) DJFMAM, and b) JJASON.

Figure 10. Global mean 6-hourly vertical profiles of CATS 1064 nm extinction for a) DJFMAM all profiles, b) DJFMAM water profiles, c) DJFMAM not-water profiles, e) JJASON all profiles, f) JJASON water profiles, g) JJASON not-water profiles.

Figure 11. Global mean 6-hourly local time (0:00 am, 6:00 am, 12:00 pm and 6:00 pm) vertical profiles of CATS 1064 nm extinction for a) DJFMAM all profiles, b) DJFMAM water profiles, c) DJFMAM not-water profiles, d) JJASON all profiles, e) JJASON water profiles, f) JJASON not-water profiles.

Figure 12. DJFMAM 6-hourly average (local time; 0:00 am, 6:00 am, 12:00 pm and 6:00 pm) vertical profiles of CATS 1064 nm for locations shown in Figure 6a; a) Africa-north, b) Middle East, c) India, and d) Northeast China.

Figure 13. JJASON 6-hourly average (local time; 0:00 am, 6:00 am, 12:00 pm and 6:00 pm) vertical profiles of CATS 1064 nm for locations shown in Figure 6b; a) Africa-north, b) Africa-south, c) Middle East, d) India, and e) Northeast China.

758

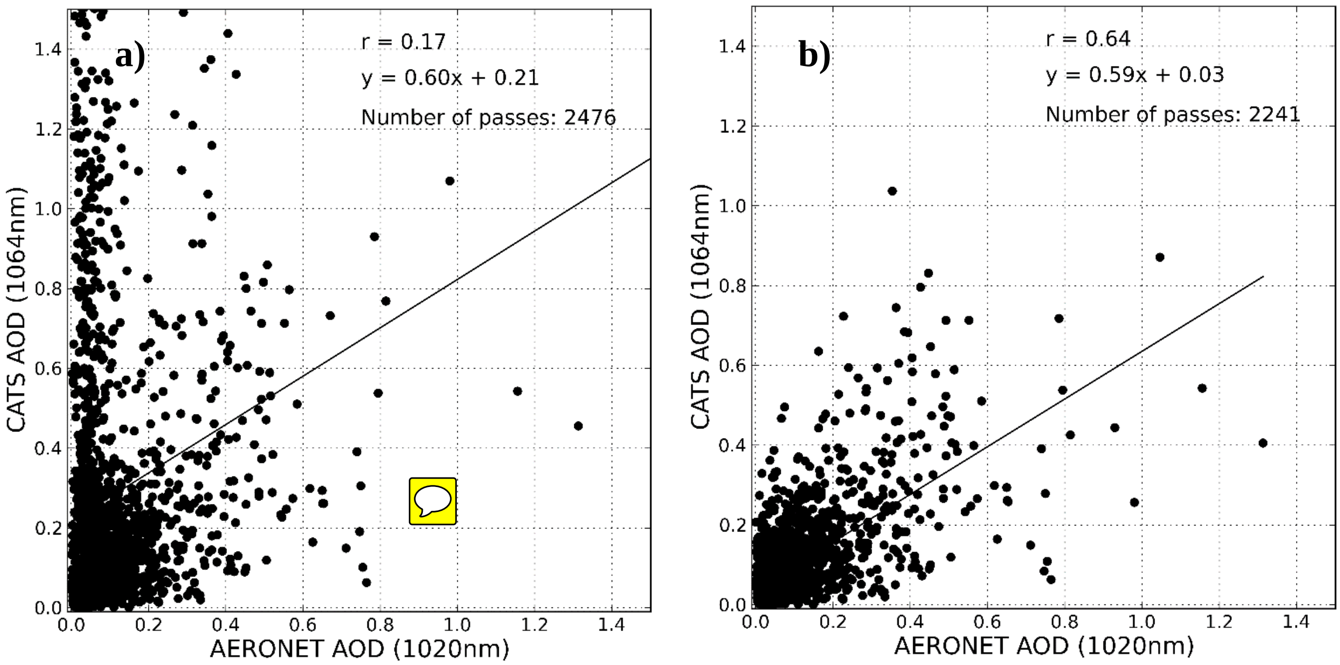

Figure 1. Collocated AERONET 1020 nm AOT vs. CATS 1064 nm AOD a) without CATS QA applied, and b) with CATS QA applied.

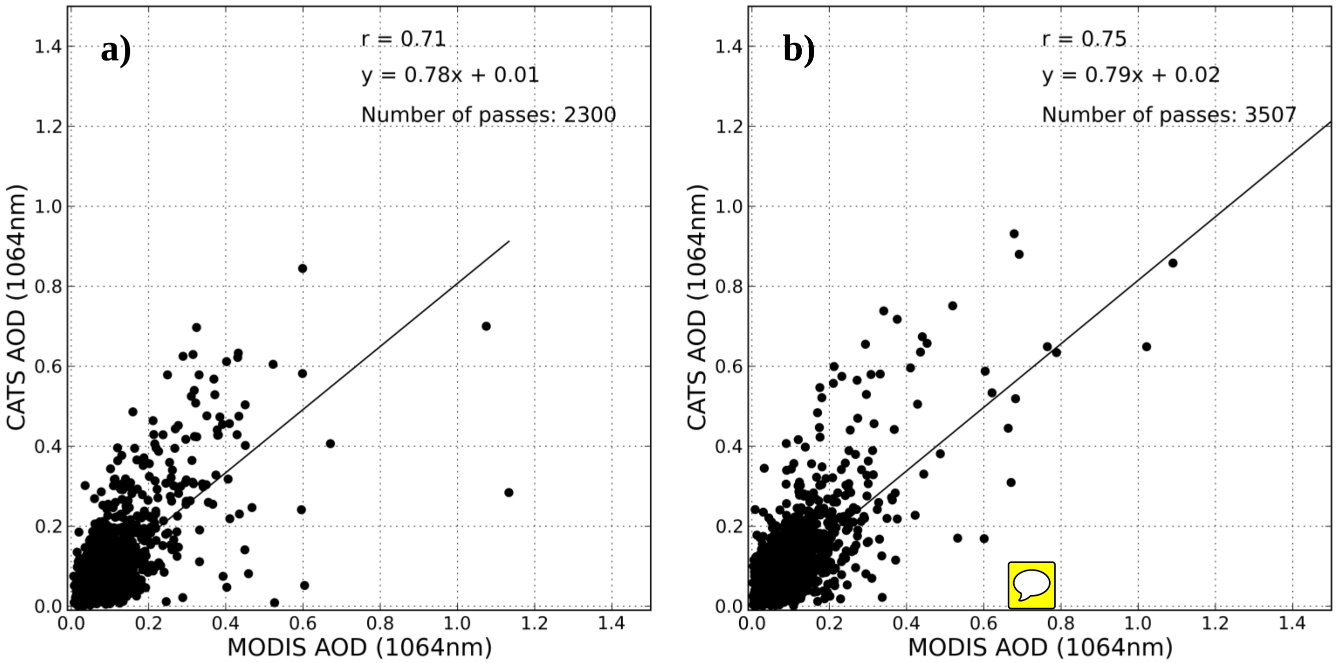

Figure 2. Collocated MODIS C6.1 a) Terra and b) Aqua estimated 1064 nm AOD vs. CATS 1064 nm AOD with CATS QA applied.

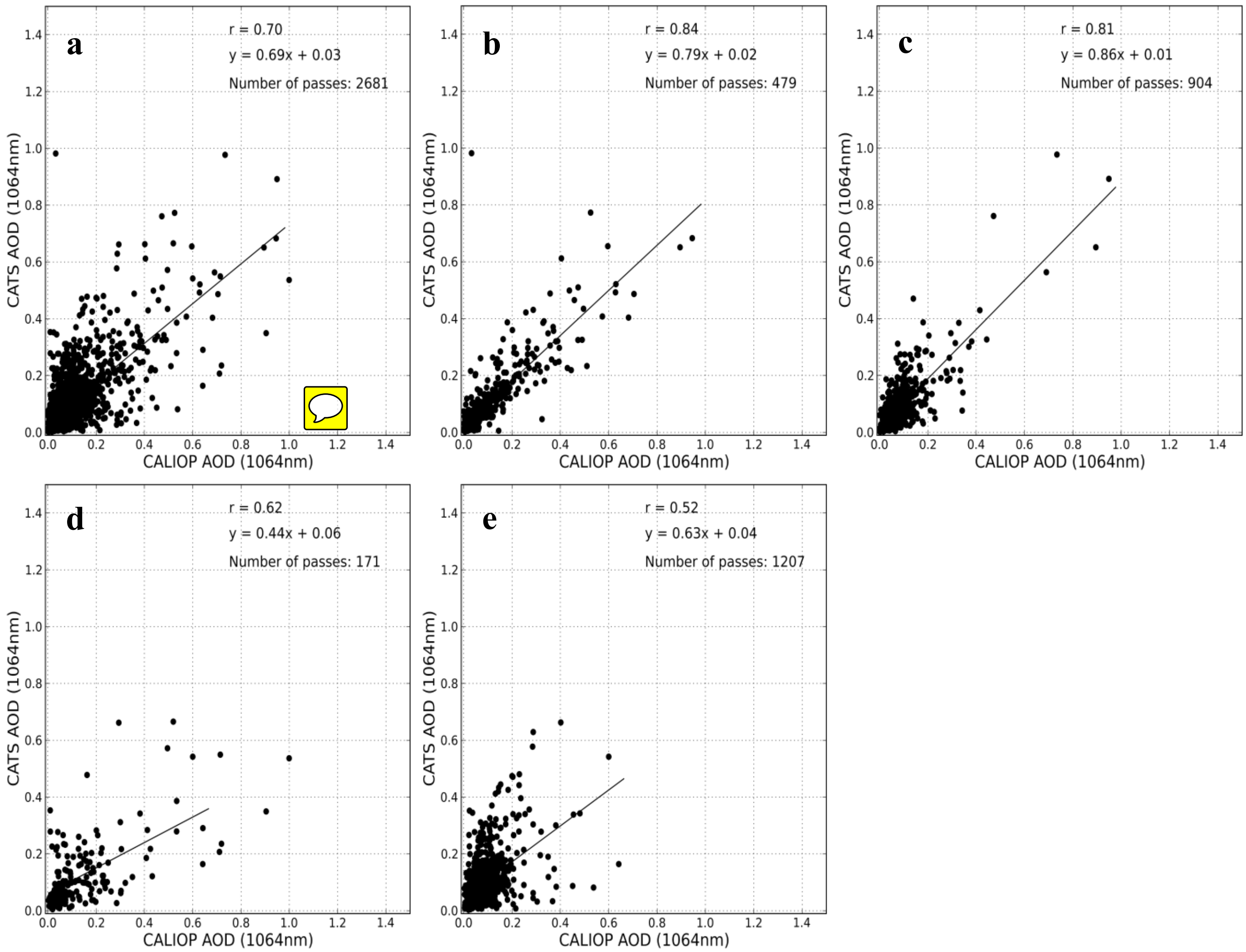

Figure 3. Collocated CALIOP 1064 nm AOD vs. CATS 1064 nm AOD with CATS QA applied for a) both day and night, b) nighttime over-land, c) nighttime over-water, d) daytime over-land, e) daytime over-water.

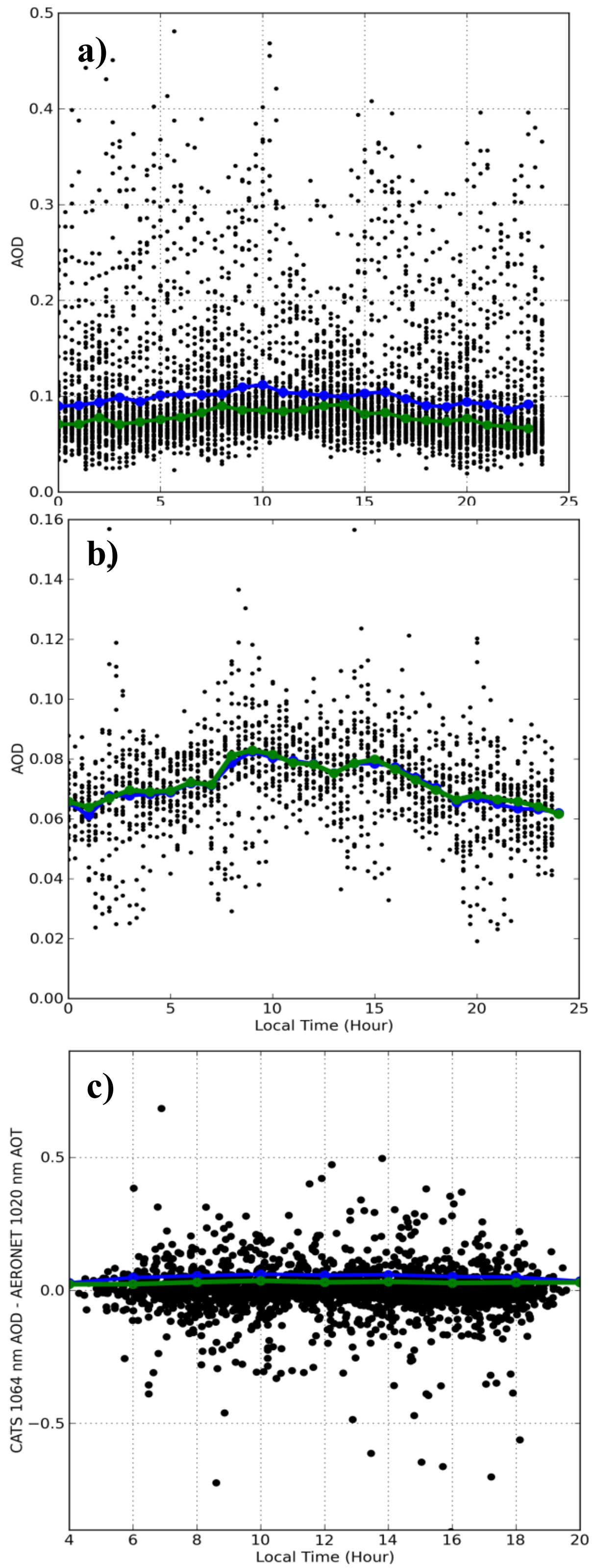

Figure 4. CATS 1064 nm AOD a) as a function of local time for the globe, and b) as a function of local time for areas south of -25 degrees. The difference between CATS 1064 nm AOD and AERONET 1020 nm AOD as a function of local time is shown in c). The mean is represented by the blue line, while the median is the green line.

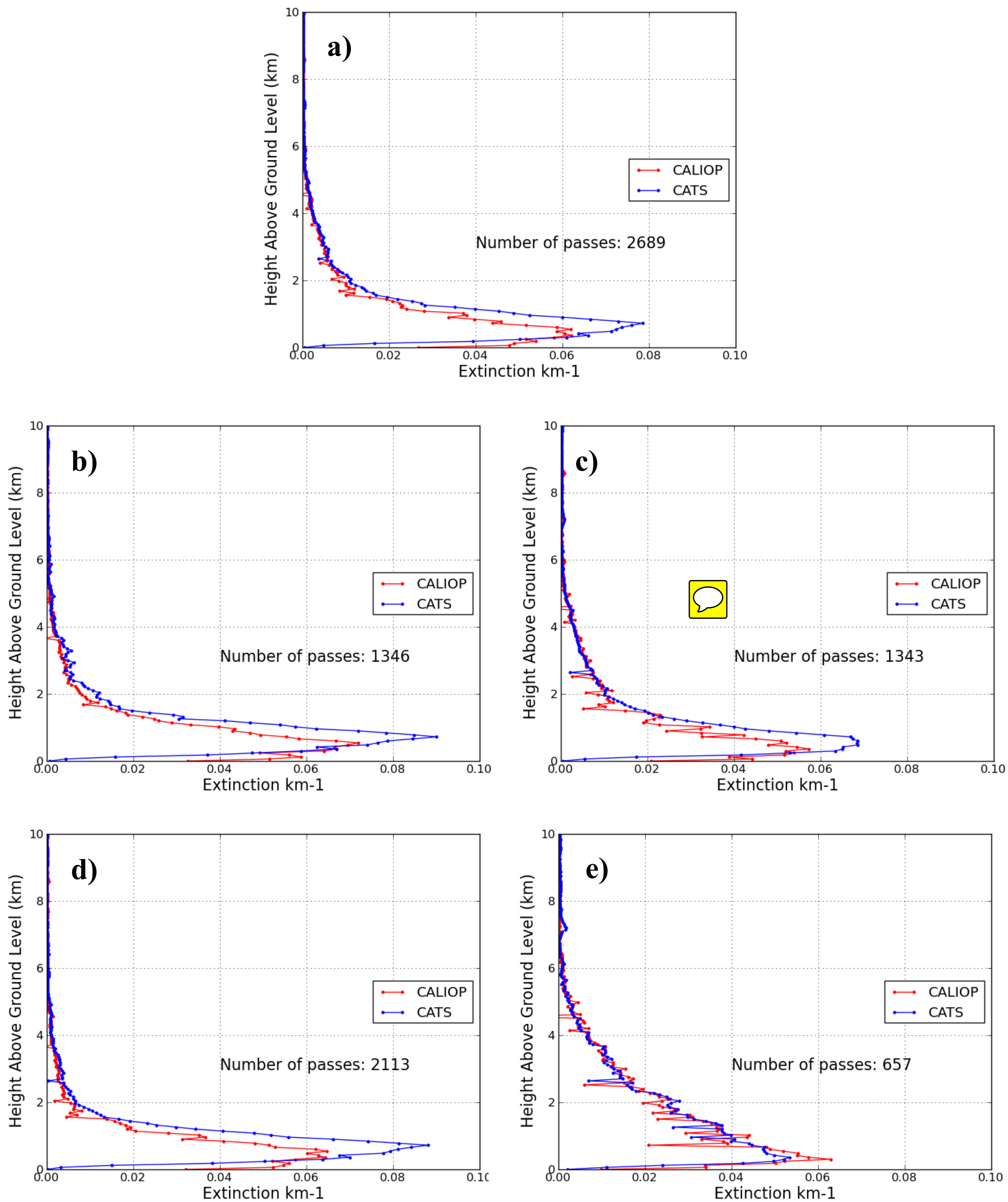

Figure 5. CATS and CALIOP vertical profiles of 1064 nm extinction for a) all profiles, b) daytime only, c) nighttime only, d) over-water, and e) over land.

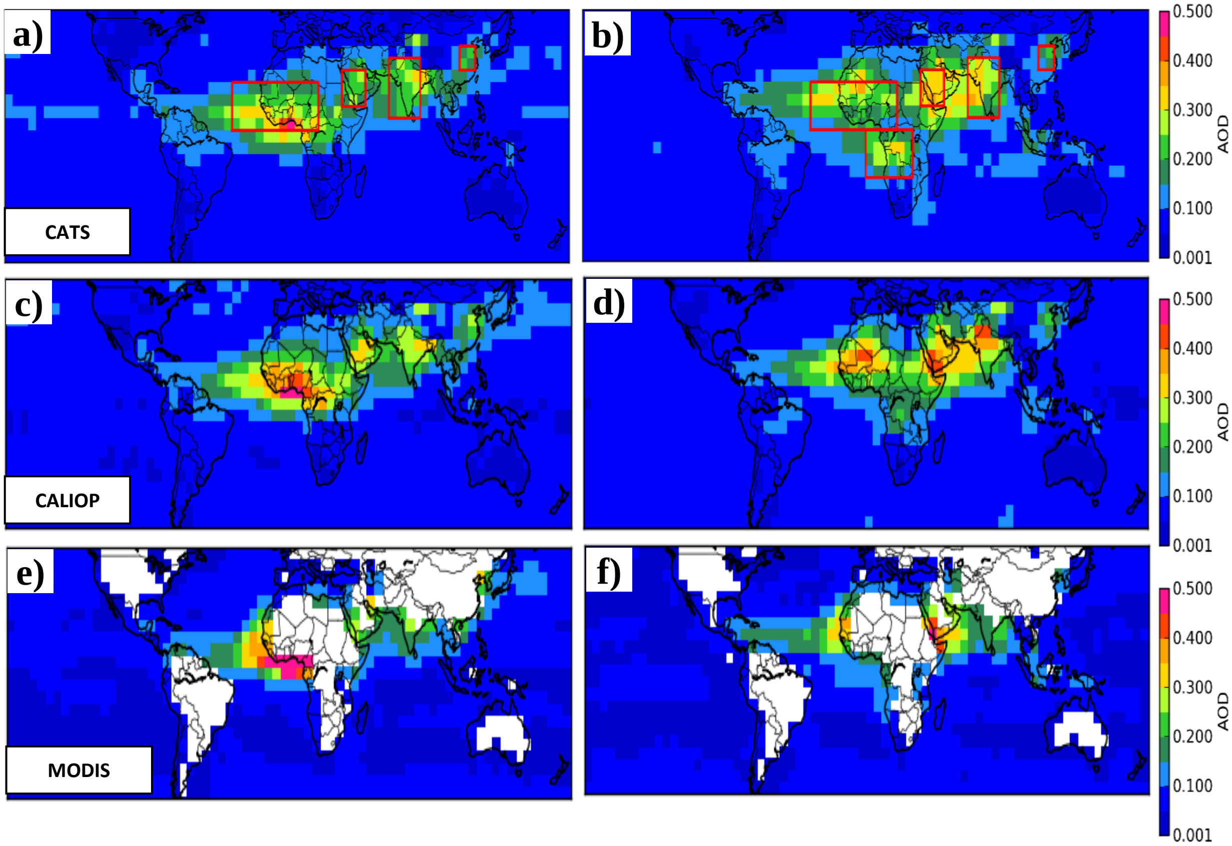

Figure 6. Mean AOD (1064 nm) by season for a) DJFMAM CATS, b) JJASON CATS, c) DJFMAM CALIOP, d) JJASON CALIOP, e) DJFMAM MODIS Aqua, and f) JJASON MODIS Aqua. Red boxes indicate locations of regional vertical distributions in Figures 12 and 13.

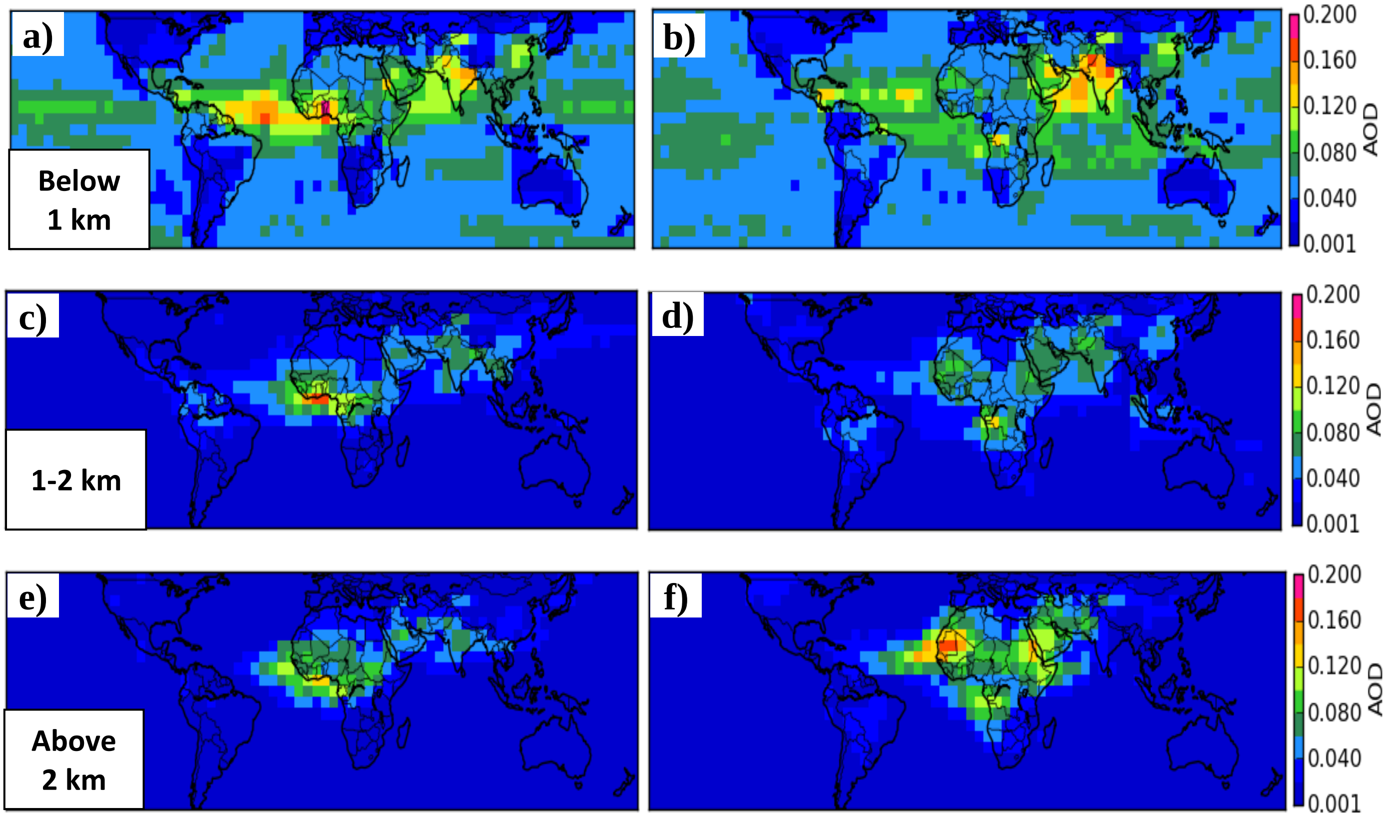

Figure 7. Mean CATS AOD (1064 nm) by season for a) DJFMAM below 1km AGL, b) JJASON below 1 km AGL, c) DJFMAM 1-2 km AGL, d) JJASON 1-2 km AGL, e) DJFMAM above 2 km AGL, and f) JJASON above 2 km AGL.

774

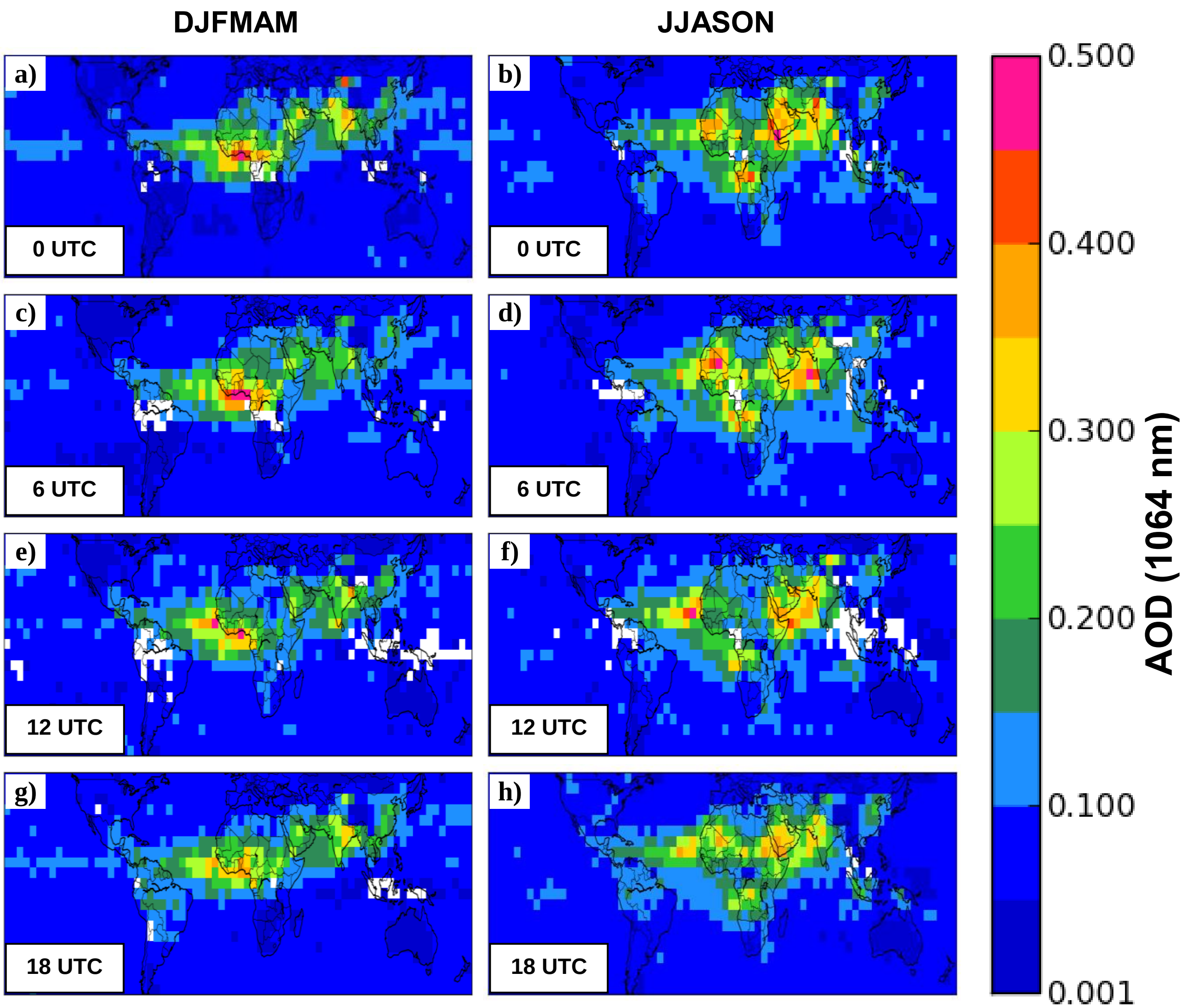

Figure 8. Seasonal Mean AOD (1064 nm) binned by every 6-hours for a) DJFMAM 0 UTC, b) JJASON 0 UTC, c) DJFMAM 6 UTC, d) JJASON 6 UTC, e) DJFMAM 12 UTC, f) JJASON 12 UTC, g) DJFMAM 18 UTC, and h) JJASON 18 UTC.

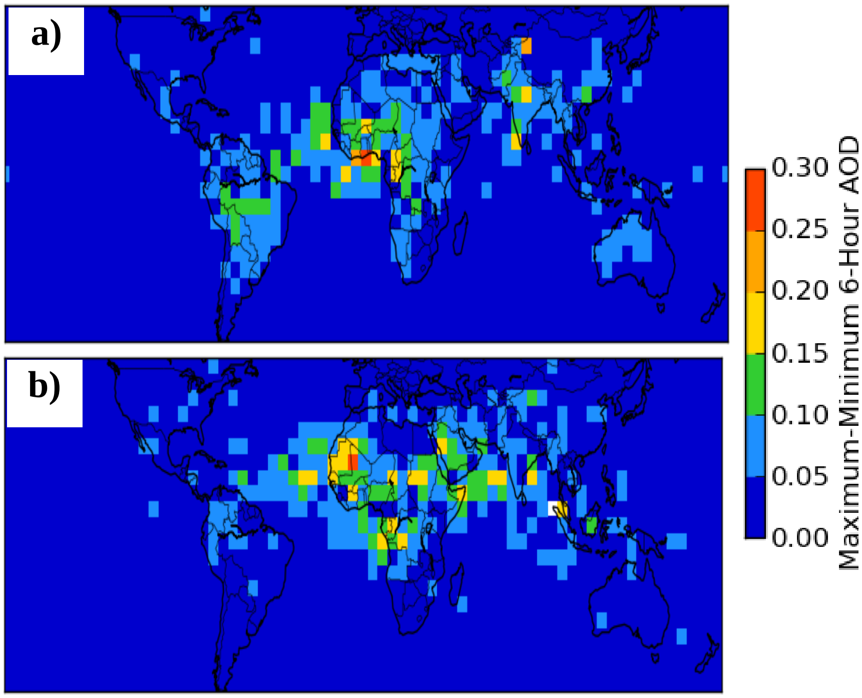

Figure 9. Maximum minus minimum mean seasonal AOD (1064 nm) for a) DJFMAM, and b) JJASON.

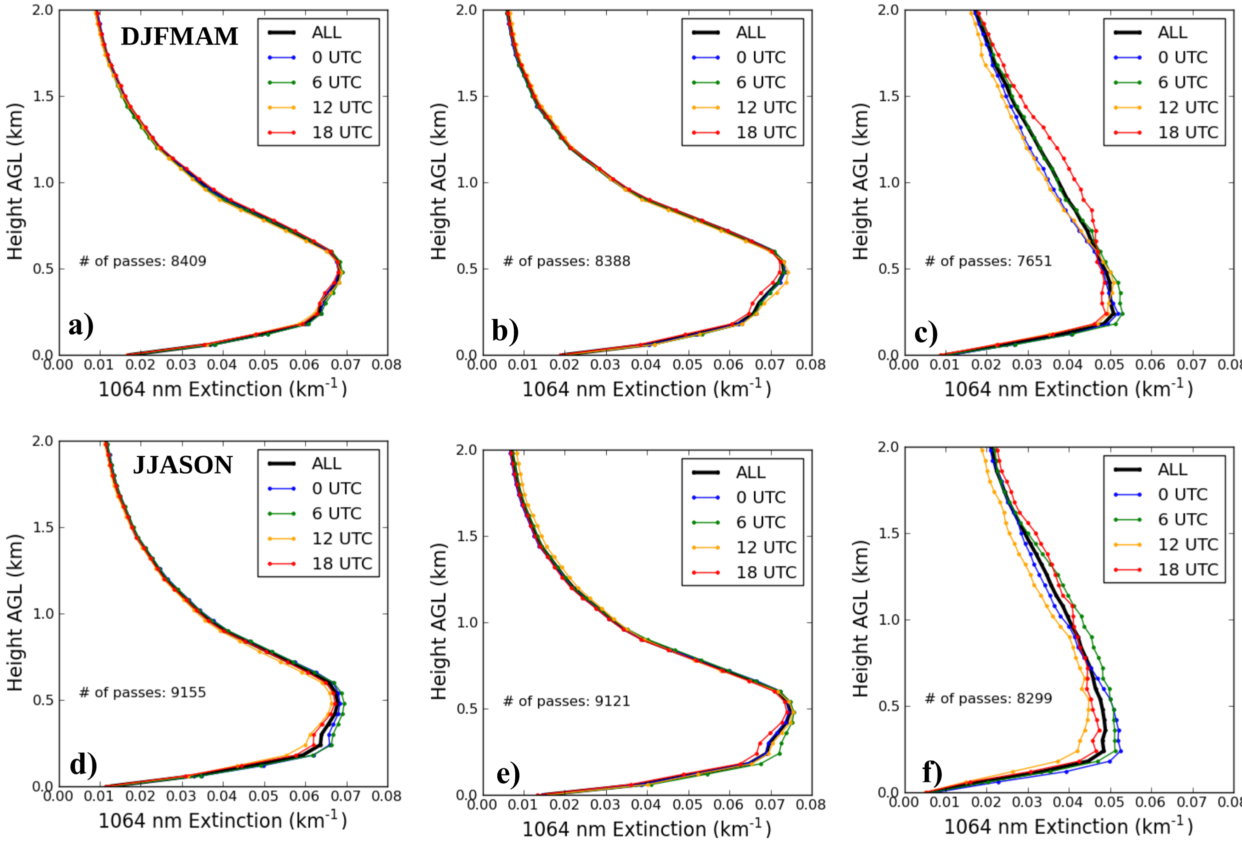

Figure 10. Global mean 6-hourly vertical profiles of CATS 1064 nm extinction for a) DJFMAM all profiles, b) DJFMAM water profiles, c) DJFMAM not-water profiles, d) JJASON all profiles, e) JJASON water profiles, f) JJASON not-water profiles.

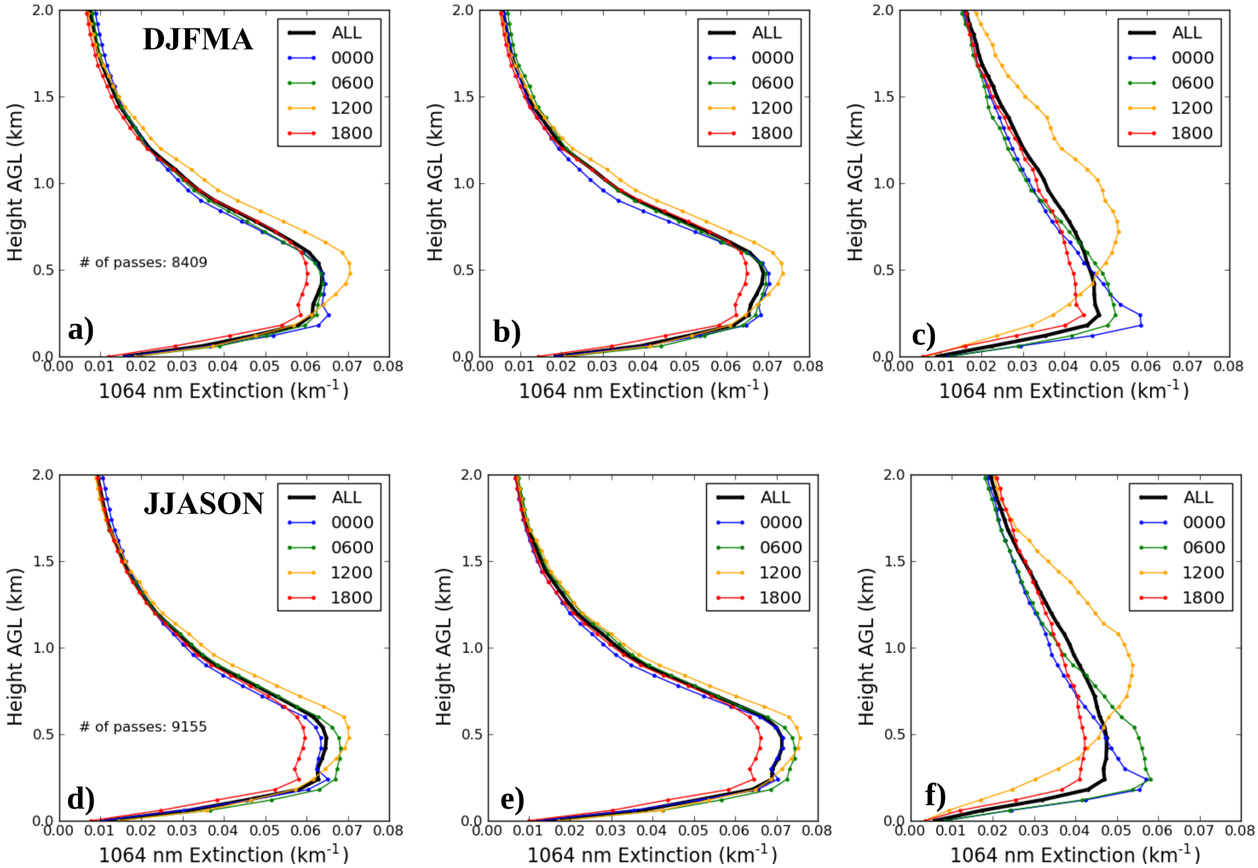

Figure 11. Global mean 6-hourly local time (0:00 am, 6:00 am, 12:00 pm and 6:00 pm) vertical profiles of CATS 1064 nm extinction for a) DJFMAM all profiles, b) DJFMAM water profiles, c) DJFMAM not-water profiles, d) JJASON all profiles, e) JJASON water profiles, f) JJASON not-water profiles.

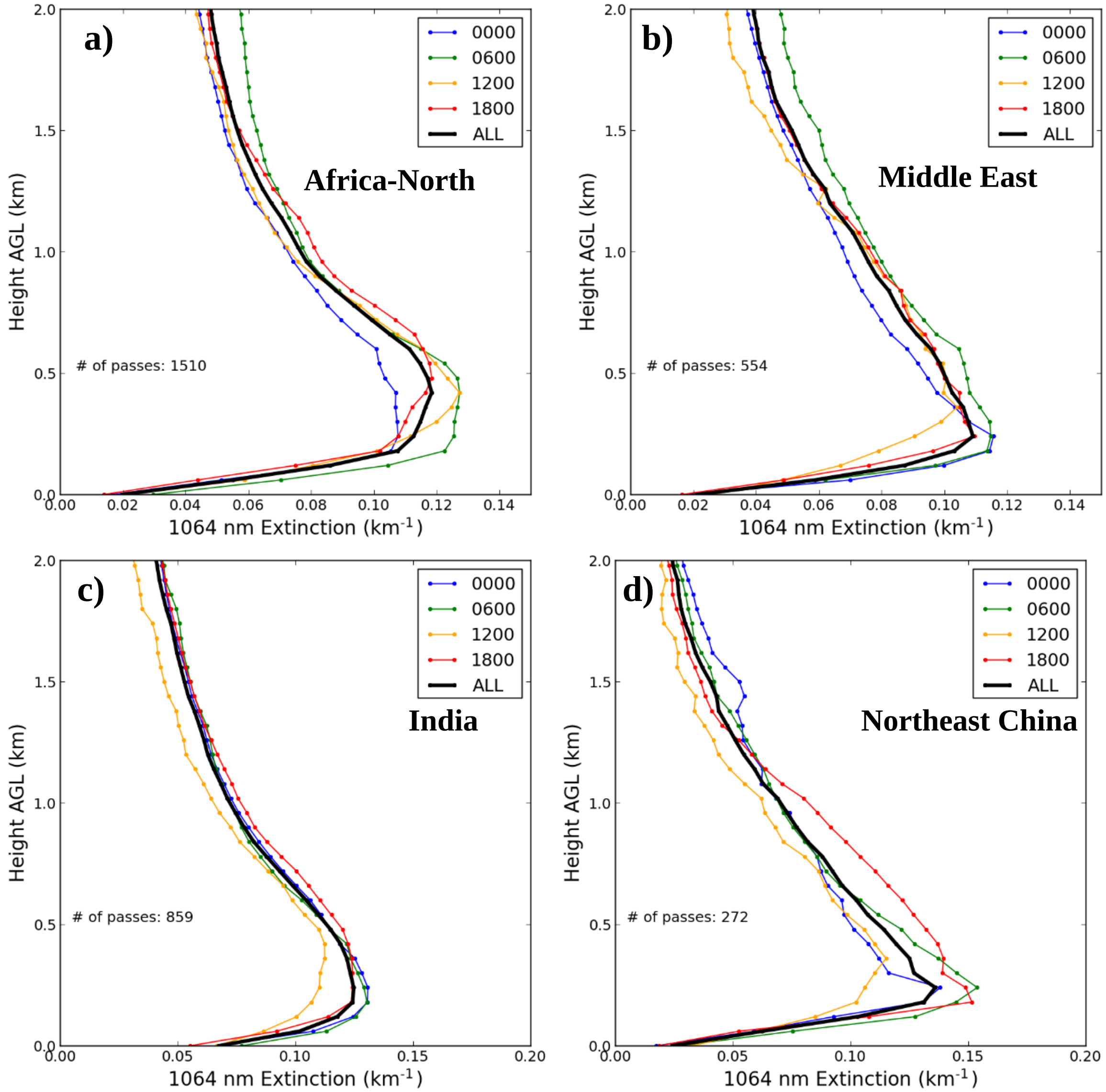

Figure 12. DJFMAM 6-hourly average (local time; 0:00 am, 6:00 am, 12:00 pm and 6:00 pm) vertical profiles of CATS 1064 nm for locations shown in Figure 6a; a) Africa-north, b) Middle East, c) India, and d) Northeast China.

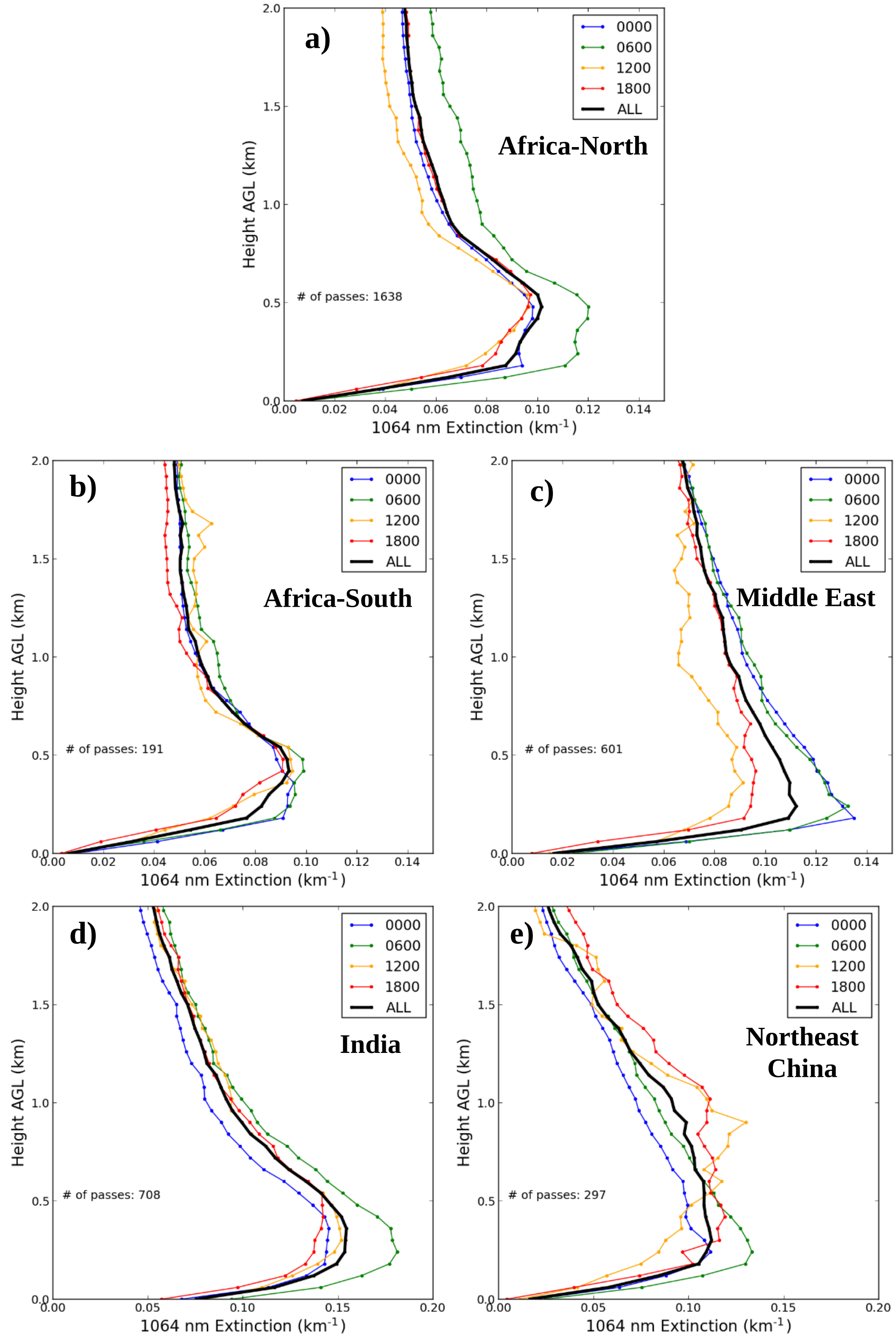

Figure 13. JJASON 6-hourly average (local time; 0:00 am, 6:00 am, 12:00 pm and 6:00 pm) vertical profiles of CATS 1064 nm for locations shown in Figure 6b; a) Africa-north, b) Africa-south, c) Middle East, d) India, and e) Northeast China.

Appendix A

The difference between CATS and CALIOP mean 1064 nm extinction for all collocated profiles as shown in Figure 5a was plotted as a function of height.

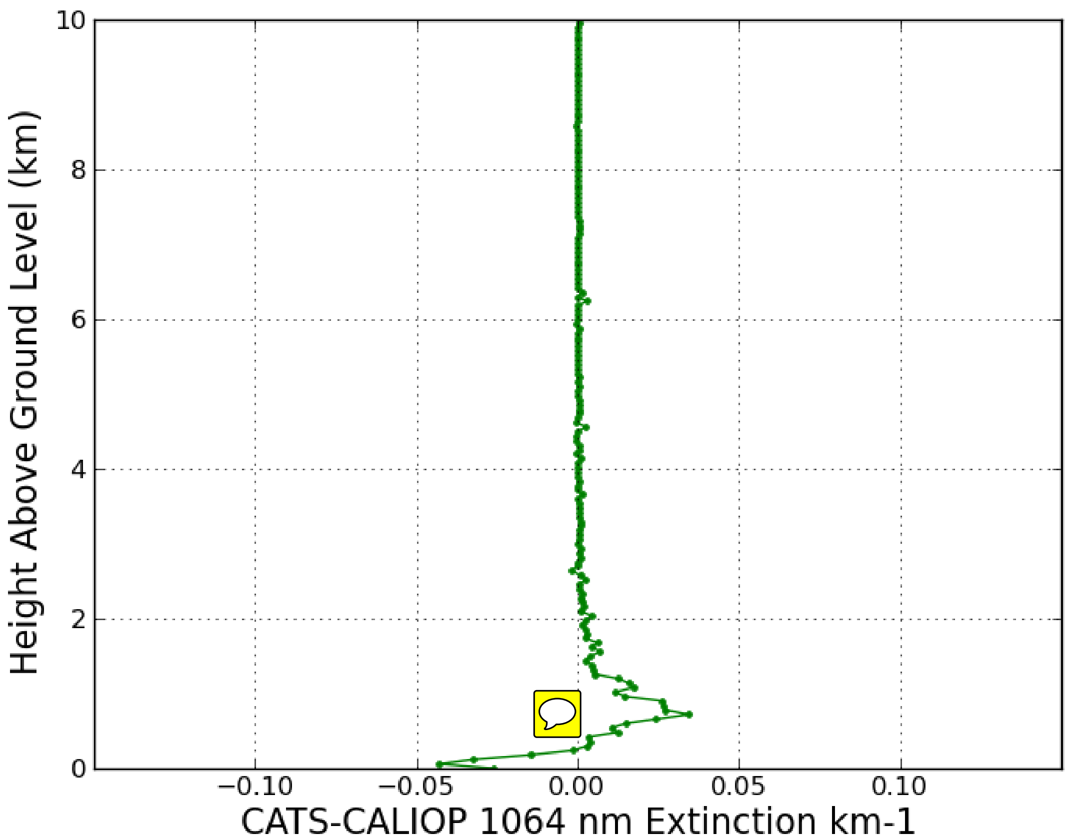

Figure A1. Difference between CATS and CALIOP mean 1064 nm extinction for all collocated profiles as a function of height.